The FASEB Journal article fj.201600398RRR. Published online October 6, 2016.

Dynamic contributions of P- and E-selectins to β_2-integrin induced neutrophil transmigration

Yixin Gong,[*,†,‡,1] Yan Zhang,[*,†,‡,§,1] Shiliang Feng,[*,†,‡] Xiaofeng Liu,[*,†,‡] Shouqin Lü,[*,†,‡,§] and Mian Long[*,†,‡,§,2]

[*]Center of Biomechanics and Bioengineering and [†]Key Laboratory of Microgravity (National Microgravity Laboratory), [‡]Beijing Key Laboratory of Engineered Construction and Mechanobiology, Institute of Mechanics, Chinese Academy of Sciences, Beijing, China; and [§]School of Engineering Science, University of Chinese Academy of Sciences, Beijing, China

ABSTRACT: Leukocyte transendothelial migration is a key step in their recruitment to sites of inflammation. However, synergic regulation of endothelium-expressed selectins on leukocyte transmigration remains unclear. In this study, an *in vitro* model was developed to investigate the dynamic contributions of P- and E-selectin to polymorphonuclear (PMN) cell transmigration under static conditions. Human umbilical vein endothelial cells (HUVECs) were treated with LPS for 4 or 12 h to induce different expression of selectins and intercellular adhesion molecule (ICAM)-1. PMN cell transmigration was increased significantly by LPS stimulation, which was higher on 4-h than on 12-h LPS-treated HUVECs. Blocking and competitive tests indicated that P-selectin engages PSGL-1 to activate β_2-integrin and initiate PMN transmigration within the first 15 min, whereas E-selectin engages CD44 to influence PMN transmigration after 15 min. P- and E-selectin–induced β_2-integrin activation is likely conducted through the spleen tyrosine kinase signaling pathway. Complicated complementary and competitive mechanisms are involved in the interaction of P-/E-selectins and their ligands to promote PMN transmigration. These results provide direct evidence of the distinct and dynamic contribution of P- and E-selectins in mediating PMN transmigration and give new insight into PMN interaction with the vessel wall.—Gong, Y., Zhang, Y., Feng, S., Liu, X., Lü, S., Long, M. Dynamic contributions of P- and E-selectins to β_2-integrin induced neutrophil transmigration. FASEB J. 31, 000–000 (2017). www.fasebj.org

KEY WORDS: PSGL-1 · CD44 · synergic mechanisms

Leukocyte transendothelial migration (TEM) is a key step in their recruitment from circulating blood to the inflamed tissue. This multistep process is presented as a cascade of successive interactions between leukocytes and endothelial cells (1). Leukocytes tether to, roll on, firmly adhere to, and crawl on the endothelium before transmigration. Several different families of adhesion molecules are involved in leukocyte–endothelium interactions (2–7).

Selectins and their ligands are essential for leukocyte extravasation during inflammation. P- and E-selectins have been shown to participate in the initial phases of this process by mediating leukocyte tethering and rolling along the vessel wall (8, 9). E-selectins are transcriptionally induced in response to the presence of inflammatory cytokines, such as IL-1β, TNF-α (10), and LPS (11) on inflamed endothelial cells and can bind to different glycosylated ligands on leukocytes, including P-selectin glycoprotein ligand (PSGL)-1, CD44, and E-selectin ligand (ESL)-1, supporting the rolling and stable arrest phenotypes of leukocytes on activated vascular endothelium (12, 13). P-selectin is stored on the membranes of platelet granules and endothelial Weibel-Palade bodies. During inflammation and thrombogenic challenge, P-selectin translocates rapidly to the cell membrane and contributes to the weak adhesion between leukocytes and stimulated endothelial cells and to the heterotypic aggregation of activated platelets and leukocytes (8). In addition to its roles in mediating tethering and rolling, E-selectins establish a direct molecular link to the cytoskeleton (14) that initiates the active crawling and transmigration of leukocytes. The binding of E- or P-selectin by specific antibodies induces an obvious rounding up of human endothelial cells. Furthermore, these antibodies trigger a transient increase in cytosolic calcium (11, 15). Thus, in addition to

ABBREVIATIONS: DIC, differential interference contrast; DPBS, Dulbecco's PBS; ESL-1, E-selectin ligand-1; FGF, fibroblast growth factor; HEPES, 4-(2-hydroxyethyl)-1-piperazineethanesulfonic acid; HUVEC, human umbilical vein endothelial cell; ICAM-1, intercellular adhesion molecule 1; PMN, polymorphonuclear; PSGL-1, p-selectin glycoprotein ligand 1; sLe^x, sialyl Lewis x; Syk, spleen tyrosine kinase; TEM, transendothelial migration

[1] These authors contributed equally to this work.

[2] Correspondence: Center of Biomechanics and Bioengineering and Key Laboratory of Microgravity (National Microgravity Laboratory), Institute of Mechanics, Chinese Academy of Sciences, No. 15 North 4th Ring Rd., Beijing 100190, China. E-mail: mlong@imech.ac.cn

doi: 10.1096/fj.201600398RRR

This article includes supplemental data. Please visit *http://www.fasebj.org* to obtain this information.

promoting the initial interaction between activated endothelium and motile leukocytes, selectins could function as signaling receptors and play a role in the induction of subsequent endothelial deformation, thereby facilitating leukocyte arrest and transmigration.

Integrins are the members of a large family of functional adhesion receptors that mediate cell–cell or cell–extracellular matrix interactions and have a pivotal role in leukocyte recruitment, phagocytosis, and immunologic synapse formation (16, 17). There are at least 3 affinity states (low-, intermediate-, and high) for β_2-integrins. Binding of β_2-integrins can be dynamically regulated by altering the affinity with a conformational change, which elevates ligand binding and reduces ligand dissociation (18, 19). Selectin and immunoreceptor engagement induce the activation of signaling pathways in leukocytes that enhance integrin affinity (inside–out signaling), whereas ligand-induced allosteric conformational changes and integrin clustering likely initiate outside–in signaling, which stabilizes adhesion and initiates transmigration (20). Recent studies have suggested that E-selectin engages PSGL-1 or CD44 through a common pathway that employs Src family kinases to induce integrin $\alpha_L\beta_2$-mediated slow leukocyte rolling (21). P-selectin binding to PSGL-1 induces an intermediate state of $\alpha_M\beta_2$ that enables interaction with ICAM-1 that promotes arrest and strengthening of adhesion (22, 23). However, the dynamic contribution of P- and E-selectins in mediating neutrophil transmigration remains unclear.

We examined the potential involvement of these adhesion molecules in PMN transmigration. Using an *in vitro* PMN transmigration assay, differential contributions of P- and E-selectins were tested to determine the dynamics of PMN transmigration. The impacts of competitive binding of CD44 and PSGL-1 to E-selectins were also investigated in the dynamic process. This type of selectin-induced β_2-integrin activation finally initiated PMN transmigration *via* specific intracellular signaling pathways. Our results provide direct evidence of dynamic contributions of P- and E-selectins to mediate PMN transmigration.

MATERIALS AND METHODS

Reagents

Human recombinant soluble E-selectin/CD62E, P-selectin/CD62P, CD44, and basic fibroblast growth factor (FGF) (146 aa) and FITC-labeled anti-ICAM-1 (BBA20) blocking mAbs were purchased from R&D Systems (Minneapolis, MN, USA). PE-labeled anti-human CD44 (BJ18), PE-labeled anti-human CD62E (HA-1f), Alexa Fluor 647–labeled anti-human CD54 (HCD54), PE-labeled anti-human CD106 (STA), PE-labeled anti-human CD11a (HI111), PE-labeled anti-human CD11b (ICRF44), PE-labeled anti-human CD162 (KPL-1) mAbs and isotype control antibody LEAF purified mouse IgG1 (MOPC-21), purified rat IgG2a (RTK2758), and LEAF purified mouse IgM (MM-30) were obtained from BioLegend (San Diego, CA, USA). Medium 199, Dulbecco's PBS, and 4-(2-hydroxyethyl)-1-piperazineethanesulfonic acid (HEPES) were obtained from GE Healthcare Life Sciences (Logan, UT, USA). Thymidine, heparin sodium salt, LPS, polybrene, piceatannol, and anti-CD11a blocking mAb (MEM25) were purchased from Sigma-Aldrich (St. Louis, MO, USA). Anti-CD11b (ICRF44) and anti-PSGL-1 (PL-1) blocking mAbs were obtained from Santa Cruz Biotechnology (Santa Cruz, CA, USA). FITC-labeled anti-E-selectin (1.2B6) and anti-CD44 (Hermes-1) blocking mAbs were purchased from Abcam (Cambridge, MA, USA). FITC-labeled anti-P-selectin blocking mAbs (AK-6) were obtained from Thermo Fisher Scientific (Waltham, MA, USA). Amphotericin B was purchased from Amresco (Solon, OH, USA), and FBS was purchased from Thermo Fisher Scientific. Anti-sLe^x blocking mAb (KM93) was a kind gift from Dr. R. P. McEver (University of Oklahoma Health Sciences Center, Oklahoma City, OK, USA).

Neutrophil isolation and preparation

Whole human blood was obtained from healthy human donors after informed consent was obtained, as approved by the Animal and Medicine Ethical Committee of the Institute of Mechanics, Chinese Academy of Sciences, in accordance with the Declaration of Helsinki. Healthy, unmedicated donors were selected randomly. PMNs were isolated from whole blood by using density gradient medium Histopaque-1119 and Histopaque-1077 (Sigma-Aldrich) (24). Isolated PMNs were washed twice with HEPES buffer [10 mM KCl, 110 mM NaCl, 10 mM glucose, 1 mM $MgCl_2$, and 30 mM HEPES (pH 7.4)] and were kept on ice in phosphate buffer with calcium and magnesium (Sigma-Aldrich until use. Isolated PMNs were used within 2 h after isolation. Neutrophil density was determined with a hand-held automated cell counter (Scepter 2.0; Merck Millipore, Darmstadt, Germany).

Cell culture, treatment, and transfection

An HUVEC line was obtained from American Type Culture Collection (ATCC, Manassas, VA, USA) and grown in Medium 199 supplemented with 20% FBS, 100 U/ml penicillin, 20 mM HEPES, 3 μg/ml thymidine, 14 U/ml heparin sodium salt, 25 μg/ml amphotericin B, and 5 ng/ml FGF. For experimental use, subcultured (passage 4) HUVECs were plated on collagen-I-coated 35 mm glass-bottomed culture dishes (Nest Scientific, Rahway, NJ, USA) to form a monolayer. To examine the potential involvement of these adhesion molecules in PMN transmigration, HUVECs were treated with LPS for 4 or 12 h to induce the expression of selectins and ICAM-1 before transmigration tests.

Immunostaining

For immunostaining experiments, HUVECs were plated on a 35 mm glass dish precoated with 20 μg/ml collagen I overnight. After treatment with LPS (1 μg/ml) for 4 or 12 h, the cells were fixed in 4% paraformaldehyde at room temperature for 10 min. After 2 washings with PBS, the collected cells were incubated with Alexa Fluor 647-anti-ICAM-1, FITC-anti-E-selectin, ,FITC-anti-P-selectin mAbs or the corresponding mouse IgG1isotype control antibodies in PBS/1% BSA for 45 min at 37°C. Images were acquired with a laser scanning confocal microscope (LSM710, Zeiss, Oberkochen, Germany) with a ×63/1.35 NA oil-immersion objective. All images were analyzed with ImageJ (National Institutes of Health, Bethesda, MD, USA).

Flow cytometry analysis

HUVECs were detached from culture dishes using 0.25% trypsin and incubated with 10 μg/ml FITC-anti-ICAM-1, PE-anti-E-selectin, FITC-anti-P-selectin mAbs or isotype-matched irrelevant antibodies in DPBS buffer on ice for 45 min. Isolated PMNs were incubated with 5 μg/ml PE-anti-human CD11a,

PE-anti-human CD11b, PE-anti-human CD44, PE-anti-human CD162 mAbs or isotype-matched irrelevant control antibodies (mouse IgG1) on ice for 45 min. After they were fully washed, HUVECs or PMNs were resuspended in DPBS and analyzed by a FACSCalibur cytometer (BD Biosciences, Franklin Lakes, NJ, USA).

Live-cell imaging

The dish containing cells was placed in a custom-made heating device that provided temperature control (37 ± 0.5°C) and a 5% CO_2 supply during imaging. All images were obtained at ×60/1.35 NA magnification with an automatic inverted microscope (IX81; Olympus, Tokyo, Japan) equipped with an electron-multiplying charge-coupled device camera (897; Andor Technologies, Belfast, United Kingdom). Time-lapse differential interference contrast (DIC) imaging was initiated when PMNs were plated onto an HUVEC monolayer, and images were acquired at 30-s intervals over a period of 60 min.

PMN adhesion and transmigration assay

Fully confluent HUVEC monolayers were treated with 1 μg/ml LPS for 4 or 12 h to induce the expression of different selectins and ICAM-1. To promote adhesion, 5×10^5 PMNs were added randomly onto the HUVEC monolayer. The fraction of neutrophil transmigration (transmigration ratio) was calculated by dividing the number of PMNs that had migrated through the endothelium at an interval of 5 min by the total number of PMNs presenting in the observation window at t = 40 min. All experiments were repeated at least 4 times.

HUVEC permeability assay

FITC-dextran (10 kDa; ThermoFisher Scientific) was used to test the permeability of the HUVEC monolayer. In brief, HUVECs were seeded at a density of 2×10^4 cells/well in 100 μl medium into the upper compartment of a 24-well Transwell (3-μm pore size; Corning Inc., Corning NY, USA). After achieving 2 d confluence, the HUVECs were treated without LPS as a control or with LPS (1 μg/ml) for 4 or 12 h, and FITC-dextran (1 mg/ml) was added to the upper compartment. After 1 h incubation, 100 μl medium was collected from the lower compartment, and fluorescence intensity was evaluated with a microplate reader (FLX800; Biotek, Winooski, VT, USA). These experiments were repeated 3 times. The data were normalized to the average fluorescence intensity of the intact HUVEC monolayer.

Numerical simulation

To better understand the dynamic contribution of P- and E-selectins to β_2-integrin-induced PMN transmigration, a theoretical model was developed, and the related numerical calculations were conducted, as described in the Supplemental Materials. In brief, the activation of β_2-integrin is controlled by the binding of P- and E-selectins with their ligands in a force-dependent manner, and the bond formation is described by a stochastic process related to the respective receptor–ligand binding kinetics. Accordingly, the dynamic features of PMN transmigration are assumed to work in the following way. The basal level of activated β_2-integrins helps PMNs to form nascent adhesions and thus induce initial cell movement. Ligand-engaged selectin bonds are strained, resulting in a stretch force that serves as an input signal for further inside–out β_2-integrin activation. Up-regulation of activated β_2-integrins further promotes focal adhesion formation, which in turn accelerates cell motion and increases the force subjected to selectin bonds.

Protein array for chemokine analysis

A human chemokine array was used to detect multiple analytes in culture supernates. HUVECs were left untreated or were treated with 1 μg/ml LPS for 4 or 12 h. The supernates were collected for chemokine analysis performed with a commercial protein array (Proteome Profiler Arrays, ARY017; R&D Systems), according to the manufacturer's instructions. Cell culture supernates (500 μl) were added to each array. Data were shown from a 5 min exposure to X-ray film (25).

Statistical analysis

All data are presented as the means ± SE. The data were compared by 1-way ANOVA followed by the Tukey *post hoc* test. All statistical analyses were performed with Prism statistical software (GraphPad Software, La Jolla, CA, USA).

RESULTS

PMN transmigration is significantly higher on 4-h LPS-treated HUVECs

PMNs were placed on top of the HUVEC monolayer to let them settle down and migrate freely along the monolayer. Subsequently, the PMNs transmigrated across the endothelium (**Fig. 1*A***), typically starting within ~5–20 min and lasting through the whole imaging course (60 min). PMN transmigration was enhanced by LPS stimulation, which was higher on 4 h than on 12-h LPS-treated HUVECs before 45 min (Fig. 1*B*). Specifically, PMN transmigration at 4-h LPS treatment took place earlier (<5 min), reached a peak at 45 min, and subsequently decreased up to 60 min. In contrast, on 12-h LPS–treated HUVECs, PMN transmigration was observed at >10 min, followed by a monotonic increase with time up to 60 min. Typical data at t = 15 and 45 min were compared, yielding a significantly higher value at 4 h than at 12 h of LPS treatment (Fig. 1*C*).

LPS is known to increase endothelial cell permeability and induce chemokine production (26, 27). To test whether differential PMN transmigration at different LPS treatment durations is attributable to these 2 factors, we first used FITC-dextran to examine the junctional permeability of the HUVEC monolayer after 4 and 12 h and with no LPS treatment. At 12 h, LPS treatment significantly enhanced HUVEC permeability over that in the other 2 conditions (Fig. 1*D*; $P < 0.0001$), whereas no differences were observed between the control and 4-h LPS treatments. These findings indicate that LPS-induced permeability alterations are unlikely to contribute to increased PMN transmigration at 4- *vs.* 12-h treatment. We also tested chemokine production from the HUVEC monolayer at 4 and 12 h with no LPS treatment. All 8 typical chemokines preserved almost the same level during the 4- and 12-h LPS treatments (Supplemental Fig. S1), excluding the possibility of chemokine-induced differential PMN transmigration at different treatment durations.

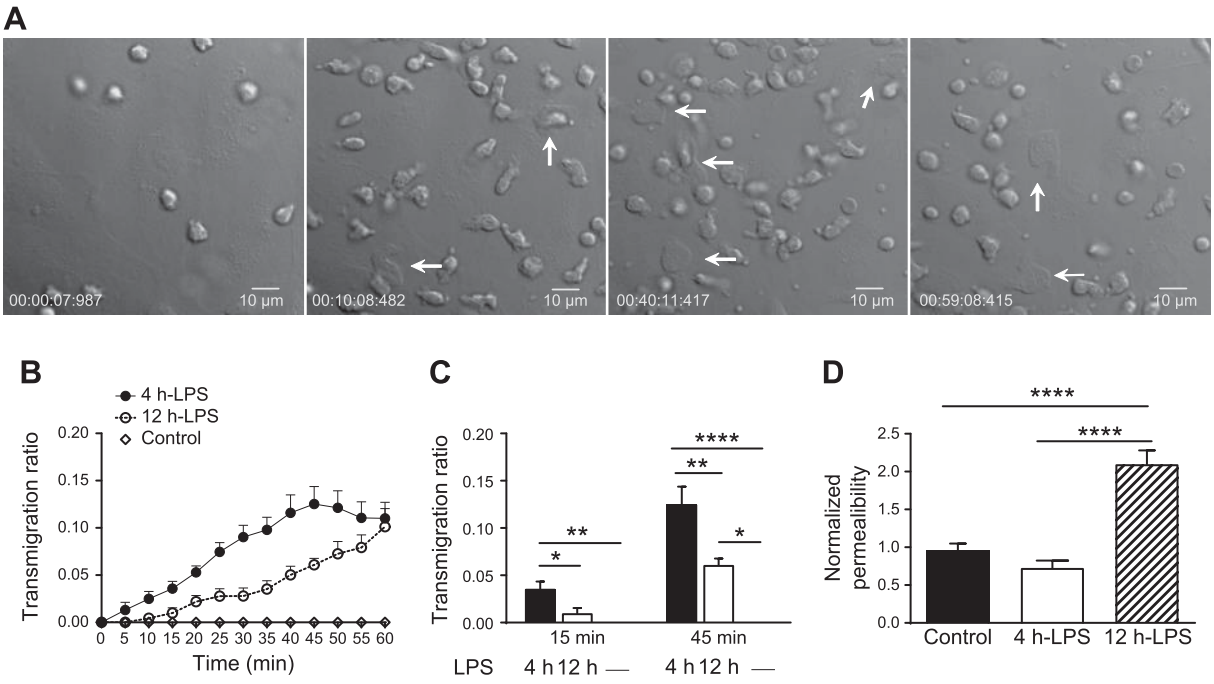

Figure 1. PMN transmigration is significantly higher on a 4-h LPS-treated HUVEC monolayer. *A*) An *in vitro* neutrophil transmigration assay was used. Representative time-lapse images are shown for PMNs migrating through the endothelium. Arrows: neutrophils that are undergoing TEM. *B*) Dynamic time courses of the PMN transmigration ratio in 4- and 12-h LPS-treated HUVECs. *C*) Typical PMN transmigration ratio in 4- and 12-h LPS-treated HUVECs at t = 15 and 45 min from *B*. *D*) HUVEC monolayer permeability assay. Data are means ± SE and are representative of 10–18 independent experiments. $^{*}P < 0.05$, $^{**}P < 0.01$, $^{***}P < 0.001$, $^{****}P < 0.0001$.

Selectin-induced β_2-integrin activation increases PMN transmigration

To further examine the potential involvement of adhesion molecules in increased PMN transmigration on the 4-h LPS-treated HUVEC monolayer, the HUVECs were exposed to 1 μg/ml LPS for 0 (control), 4, 8, and 12 h. Flow cytometry analysis (**Fig. 2*A*, *B***) and immunostaining (Supplemental Fig. S2) were used to measure E-selectin, P-selectin, and ICAM-1 expression. Compared to control cells (no LPS treatment), E-selectin expression peaked (more than 10-fold) at 4 h (Fig. 2*B*) and then declined to baseline within 12 h. P-selectin expression on 4-h LPS treatment increased by ~30% and returned to baseline within 12 h. By contrast, ICAM-1 expression increased with increasing LPS treatment duration and reached a plateau beyond 8 h. These data present distinct expression dynamics for different adhesive molecules, as expected (11).

Activation of β_2-integrin is known to mediate PMN rolling and adhesion on endothelium (22, 28). To test whether β_2-integrins are responsible for increased PMN transmigration on a 4-h LPS-treated HUVEC monolayer, we also examined the expression of CD11a/CD18 and CD11b/CD18 on PMNs, yielding stable presentation of β_2-integrins on the PMN surface (Fig. 2*C*). We then tested PMN transmigration dynamics on the HUVEC monolayer by treating PMNs with β_2-integrin blocking or activating antibodies (**Fig. 3*A*–*D***). Incubation of the PMNs with anti-CD11a (MEM25) and anti-CD11b (ICRF44) blocking mAbs lowered dramatically the transmigration ratio onto the 4-h LPS-treated HUVEC monolayer to the level of 12-h treatment. By contrast, incubation of PMNs with β_2-integrin–activating mAbs (MEM48) enhanced the transmigration ratio on the 12-h LPS-treated HUVEC monolayer to the level observed after 4-h treatment. This antibody-induced inhibition or activation is specific because incubation with isotype-matched irrelevant mAbs had no effect (Fig. 3*A*, *B*). These results indicate that activated β_2-integrin is responsible for increased transmigration on a 4-h *vs.* 12-h LPS-treated HUVEC monolayer.

We further performed cross tests by adding PMNs incubated with MEM25 and ICRF44 to a 12-h LPS-treated HUVEC monolayer and by adding PMNs incubated with MEM48 to a 4-h LPS-treated monolayer. The PMN transmigration ratio on the 12- or 4-h LPS-treated HUVEC monolayer did not decrease or increase any further when β_2-integrin was blocked (CD11a and CD11b) or activated (Fig. 3*C*, *D*), suggesting that β_2-integrins were in an activated state after PMNs were placed on 4-h LPS–treated HUVEC monolayer and those inactive β_2-integrins contributed much less to PMN transmigration on 12-h LPS–treated HUVECs. Because ligand-engaged P- or E-selectin can activate β_2-integrin in a spleen tyrosine kinase (Syk)–dependent manner (29, 30), we simply assumed that P- and E-selectin-induced β_2-integrin activation was responsible for the increased PMN transmigration on the 4-h LPS–treated HUVEC monolayer. Using piceatannol, but not DMSO, to inhibit β_2-integrin activation through the Syk/Btk signaling pathway significantly decreased PMN transmigration on 4-h LPS treatment (Fig. 3*E*, *F*), which supported the assumption. Taken together, these

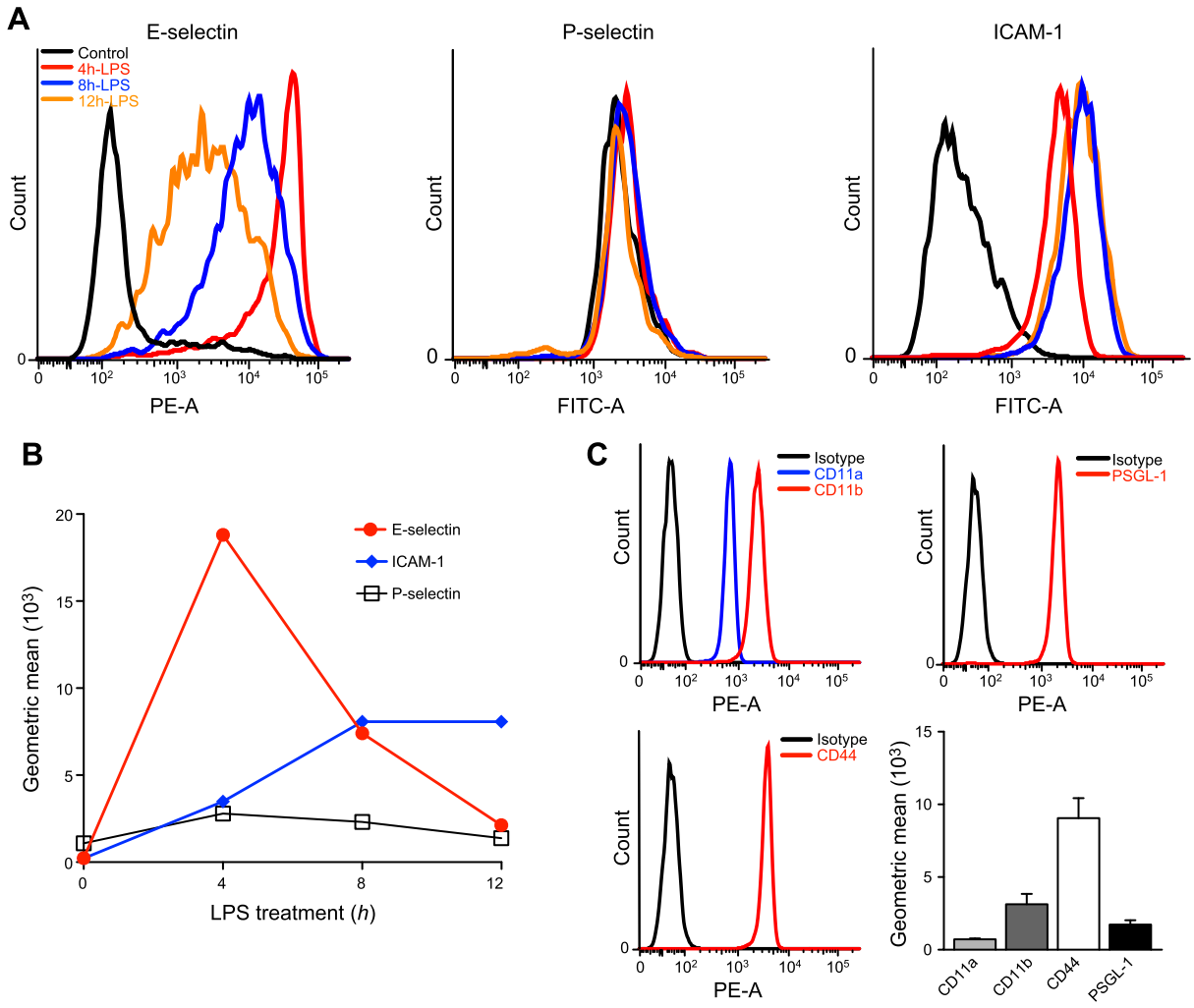

Figure 2. Cellular adhesion molecules are expressed dynamically on LPS-treated HUVECs or intact PMNs. *A*) HUVEC monolayers treated for 4, 8, and 12 h with LPS or not treated (control) were collected and then stained with respective mAbs. Flow cytometry analysis was used to determine E-selectin, P-selectin, and ICAM-1 expression. *B*) Time courses of E-selectin, P-selectin, and ICAM-1 expression on HUVECs exposed to LPS treatment. Data were collected from 6 independent experiments. *C*) Expression of CD11a, CD11b, CD44, and PSGL-1 on PMNs measured by flow cytometry analysis. PMNs incubated with FITC-conjugated isotype-matched mAbs were used as the control. Data were collected in 3–4 independent experiments.

results suggest that P- and E-selectin-induced β_2-integrin activation was responsible for increased PMN transmigration on the 4- *vs.* the 12-h LPS-treated HUVEC monolayer.

Dynamic contributions of E- and P-selectin during PMN transmigration

To further elucidate the dynamic contributions of P- and E-selectin-induced β_2-integrin activation, we tested molecular mechanisms for 2 physiologic selectin ligands on the PMN surface, PSGL-1 and CD44, where PSGL-1 binds to P- and E-selectins (31) and CD44 serves as an E-selectin ligand (32, 33). PSGL-1 and CD44 were highly expressed on human PMNs (Fig. 2*C*). Thus, HUVEC-expressed P- and E-selectins competitively bind to PSGL-1 on PMNs, whereas PSGL-1 and CD44 on PMNs competitively bind to HUVEC E-selectin. To isolate the independent contributions of P-selectin–PSGL-1 binding to PMN transmigration on the 4-h LPS-treated HUVEC monolayer, we first used saturated (5 μg/ml) (17) soluble CD44 to competitively bind to E-selectin on the HUVECs and then added PMNs onto the HUVECs and measured the isolated contribution of P-selectin–PSGL-1 binding to PMN transmigration (**Fig. 4*A*, *B***). Next, we applied saturated soluble P-selectin (5 μg/ml), which competitively bound to PSGL-1 on the PMNs, to isolate the independent contribution of E-selectin–CD44 binding (Fig. 4*C*, *D*). Finally, we simultaneously added the P-selectin-blocking mAb G1 onto the HUVECs and the anti-CD44-blocking mAb Hermes-1 to the PMNs to isolate the independent contribution of E-selectin–PSGL-1 binding where IgG2a and IgG1 served as the isotype-matched control (Fig. 4*E*, *F*).

Independent contributions observed for P-selectin–PSGL-1 (Fig. 4*A*) and E-selectin–PSGL-1 (Fig. 4*E*) binding were similar, given that either supported the same PMN transmigration dynamics on the 4-h LPS-treated HUVEC monolayer and yielded a higher ratio, typically at t = 15 and 45 min than those on the 12-h LPS-treated

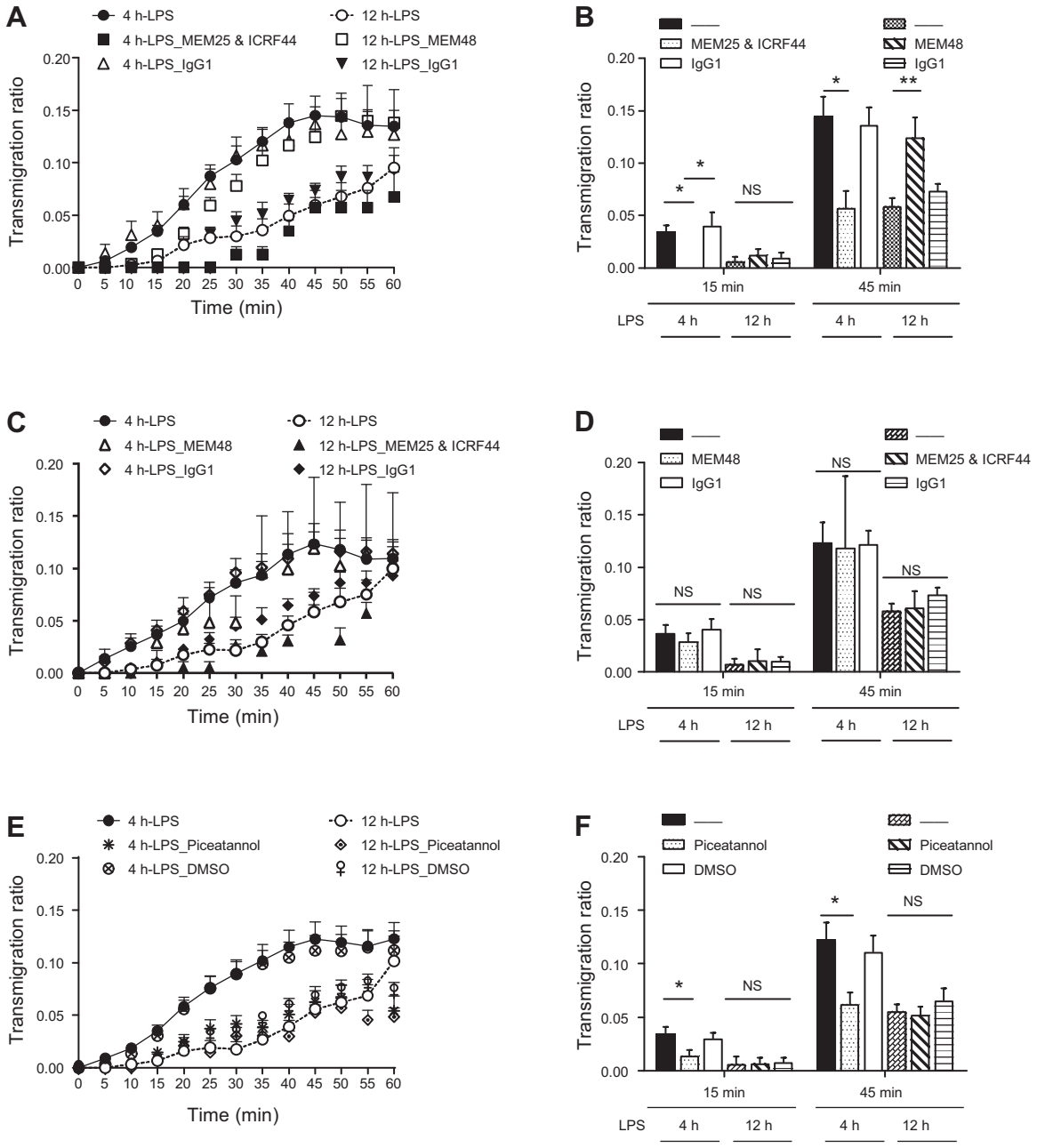

Figure 3. High selectin expression correlates with β_2-integrin activation for increased PMN transmigration on a 4-h LPS-treated HUVEC monolayer. *A*) Dynamic time courses of the transmigration ratio for PMNs incubated with anti-CD11a (MEM25) and anti-CD11b (ICRF44) mAbs on a 4-h LPS-treated HUVEC monolayer, or with a β_2-integrin activation mAb (MEM48) on a 12-h LPS-treated HUVEC monolayer. Isotype-matched irrelevant mAbs (IgG1) were used as the control. Data were collected in 6–16 independent experiments. *C*) Dynamic time courses of the transmigration ratio for PMNs incubated with the MEM25 and ICRF44 mAbs on a 12-h LPS-treated HUVEC monolayer or with MEM48 mAb on a 4-h LPS-treated HUVEC monolayer. An isotype-matched irrelevant mAb (IgG1) was used as the control. Data were collected in 4–17 independent experiments. *E*) Dynamic time courses of the transmigration ratio for PMNs incubated with piceatannol to inhibit β_2-integrin activation through the Syk/Btk signaling pathway. DMSO served as the vehicle control. Data were collected in 6–15 independent experiments. Data for 4- or 12-h LPS treatment are also presented in *A*, *C*, and *E* for comparison. *B*, *D*, *F*) Typical PMN transmigration ratio at $t = 15$ and 45 min from *A*, *C*, and *E* were compared using 1-way ANOVA, followed by Tukey *post hoc* test. Data are means ± SE. $^*P < 0.05$, $^{**}P < 0.01$.

monolayer (Fig. 4*B*, *F*).When soluble P-selectin was used to compete with PSGL-1 on the PMNs (Fig. 4C), the transmigration ratio was similar to that at $t = 45$ min (Fig. 4*D*) but significantly lower at $t = 15$ min than that on 4-h LPS treatment, indicating that the binding of E-selectin–CD44 initiated PMN transmigration 15 min later compared with P- or E-selectin binding to PSGL-1. Taken together, these data suggest that P- and E-selectins engaged PSGL-1 to activate β_2-integrin and to influence PMN transmigration immediately after their addition onto HUVECs, and E-selectin engaged CD44 to activate β_2-integrin and to influence

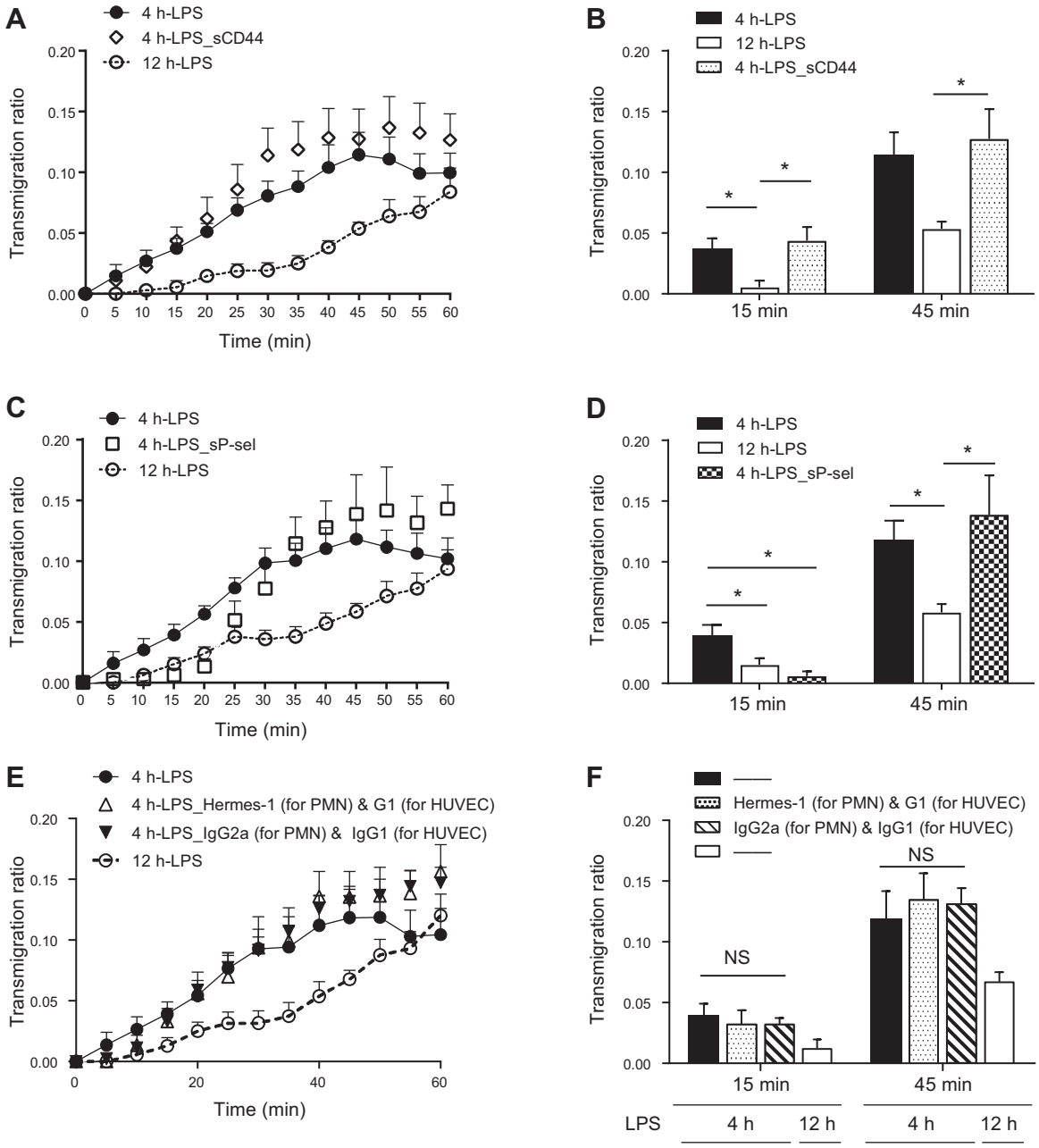

Figure 4. Dynamic contributions of E- and P-selectin to PMN transmigration. *A*) Dynamic time course of the transmigration ratio for PMNs on a 4-h LPS-treated HUVEC monolayer incubated with 5 μg/ml soluble (s)CD44. Data were collected in 12–16 independent experiments. *C*) Dynamic time courses of the transmigration ratio for PMNs incubated with soluble P-selectin (sP-sel) on a 4-h LPS-treated HUVEC monolayer. Data were collected in 6–15 independent experiments. *E*) Dynamic time courses of the transmigration ratio for PMNs incubated with the anti-CD44 blocking mAb Hermes-1 on a 4-h LPS-treated HUVEC monolayer incubated with the anti-P-selectin blocking mAb G1. Isotype-matched irrelevant mAbs (IgG2a and IgG1) were used as controls. Data were collected in 10–15 independent experiments. Data for 4- or 12-h LPS treatment are also presented in *A*, *C*, and *E* for comparison. *B*, *D*, *F*) Typical PMN transmigration ratio at $t = 15$ and 45 min from *A*, *C*, and *E* were compared using 1-way ANOVA, followed by Tukey *post hoc* test. Data are means ± SE. $^*P < 0.05$.

PMN transmigration only 15 min after their addition onto HUVECs.

Complementary and competitive roles of P-/E-selectin–ligand pairs in PMN transmigration

The above data suggest that both PSGL-1 and CD44 are involved in the capability of P- and E-selectin to enhance PMN transmigration. However, blocking CD44 (**Fig. 5*A, B***) or P-selectin alone (Fig. 5*E, F*) did not have a significant effect on PMN transmigration, suggesting that selectin–ligand pairs complemented each other very well to promote increased PMN transmigration on 4-h LPS treatment. By contrast, blocking PSGL-1 alone significantly lowered PMN transmigration, especially before 15 min (Fig. 5*C, D*), indicating that the binding of P-/E-selectin to

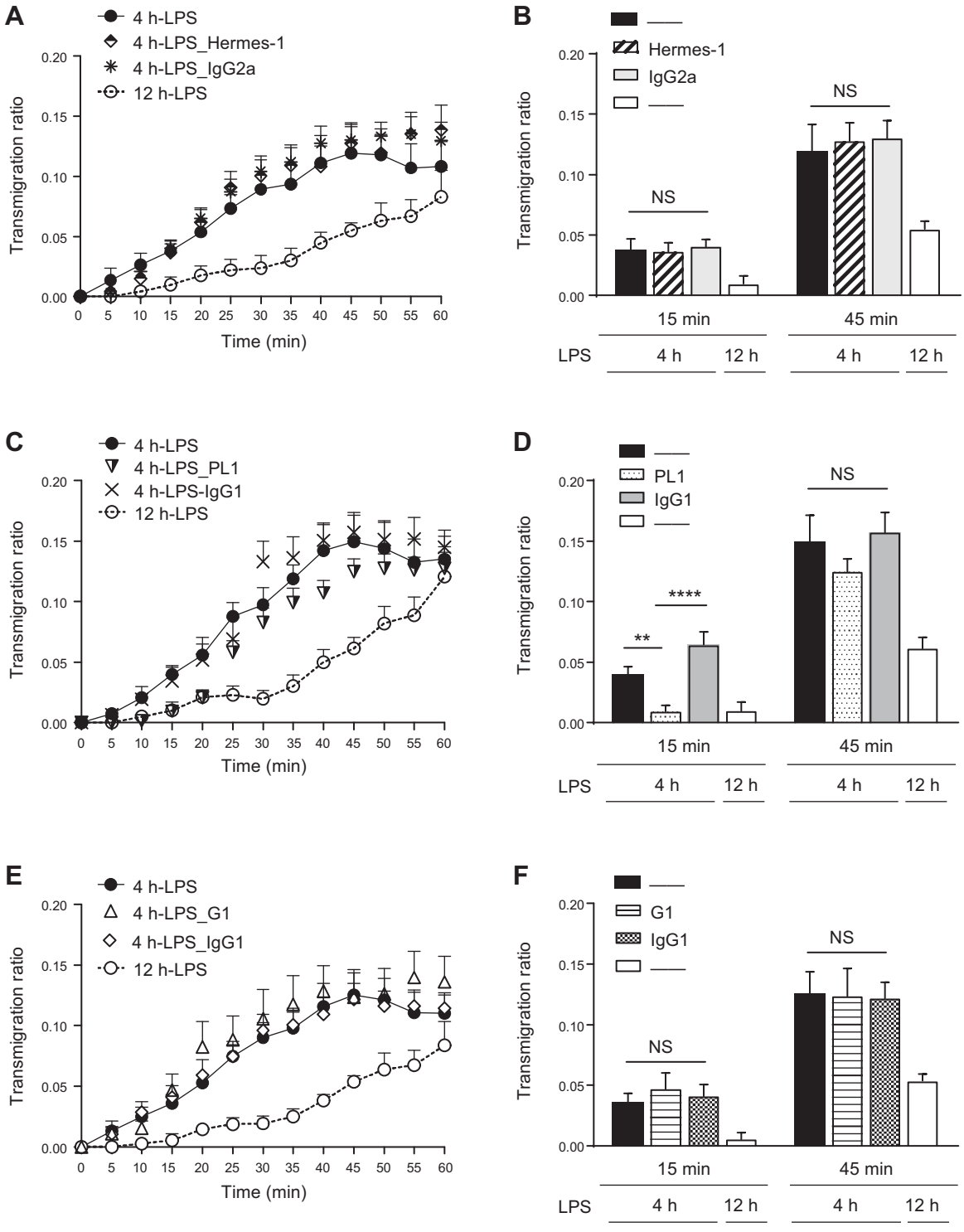

Figure 5. Distinct dynamics of antibody blocking on PMN transmigration. *A*) Dynamic time course of transmigration ratio for PMNs incubated with the anti-CD44 blocking mAb Hermes-1 on a 4-h LPS-treated HUVEC monolayer. An isotype-matched irrelevant mAb (IgG2a) was used as the control. Data were collected in 11–21 independent experiments. *C*) Dynamic time courses of the transmigration ratio for PMNs incubated with the anti-PSGL-1 blocking mAb PL1 on a 4-h LPS-treated HUVEC monolayer. An isotype-matched irrelevant mAb (IgG1) was used as the control. Data were collected in 7–18 independent experiments. *E*) Dynamic time course of the transmigration ratio for PMNs on a 4-h LPS-treated HUVEC monolayer incubated with the anti-PSGL-1 blocking mAb PL1. Data were collected in 12–18 independent experiments. An isotype-matched irrelevant mAb (IgG1) was used as the control. Data for 4- or 12-h LPS-treatment are also presented in *A*, *C*, and *E* for comparison. *B*, *D*, *F*) Typical PMN transmigration ratio at $t = 15$ and 45 min from *A*, *C*, and *E* were compared using 1-way ANOVA, followed by Tukey *post hoc* test. Data are means ± SE. $^{**}P < 0.01$, $^{****}P < 0.0001$.

PSGL-1 plays a dominant role in mediating PMN transmigration, as compared to E-selectin–CD44 binding. These results imply that a complicated network of molecular interactions activate β_2-integrin and then enhance PMN transmigration. To better understand the dynamic contribution of P- and E-selectin to β_2-integrin induced PMN transmigration, we conducted theoretical analyses to determine the time-dependent evolution of the amount of activated β_2-integrin that correlates positively with PMN transmigration (see Supplemental Materials). Numerical simulations agreed well with the experimental data for their complementary and competitive roles to induce β_2-integrin activation (Supplemental Fig. S4). Specifically, on the one hand, every selectin-engaged binding (*i.e.*, P-selectin–PSGL-1, E-selectin–PSGL-1, or E-selectin–CD44) can induce β_2-integrin activation independently at a confined intensity. Higher affinity of P- and E-selectin to PSGL-1 binding promotes a high force exerted on the selectin-PSGL-1 bond, which is more likely to exceed the threshold force and in turn leads to more effective β_2-integrin activation *via* the inside–out signaling pathway (*i.e.*, the Syk pathway in the current study) (Supplemental Fig. S4*A*). On the other hand, the probability that the force exerted on E-selectin-CD44 bond with lower binding affinity exceeds the threshold force is too low to induce β_2-integrin activation efficiently (Supplemental Fig. S4*B*). Although the expression level of P-selectin is much lower than that of E-selectin, the highest affinity of P-selectin–PSGL-1 binding may also induce efficient activation of β_2-integrin. With E- and P-selectin coexpression, β_2-integrin activation displayed little variation, suggesting that the activation rate of β_2-integrin had reached to the upper limit level during the sole expression of P-selectin (Supplemental Fig. S4*A*). In the case of PSGL-1 and CD44 coexpression, both CD44 and PSGL-1 may compete with the limited E-selectins. The on-rate of PSGL-1 binding with E-selectin is decreased by competing CD44. However, the activation of β_2-integrin is not affected because of the limitation of intracellular signaling strength (Supplemental Fig. S4*B*). We also tested the competition of these molecules by predicting the absolute number of engaged receptor–ligand bonds using the parameters listed in Supplemental Table S1. Numerical simulations indicated that both PSGL-1 and CD44 compete to bind to E-selectin (Supplemental Fig. S5*A*, *B*) but no competition exists for E- and P-selectin binding to PSGL-1 (Supplemental Fig. S5*C*, *D*), which is mainly attributable to the outnumbered PSGL-1 or CD44 density, as compared to the density of E- and P-selectin. Taken together, these simulations supported the complementary and competitive roles of P- and /E-selectin–ligand pairs in PMN transmigration.

Intracellular signaling complexity in selectin-engaged β_2-integrin activation and then PMN transmigration enhancement was further observed from our simple double-blocking tests. That blocking both PSGL-1 and CD44 did not completely block PMN transmigration (**Fig.6*A, B***; decreased to the same level as that on 12-h LPS treatment) suggests that selectin-engaged β_2-integrin activation is only specific for the increased PMN transmigration on 4-h LPS-treatment. Blocking sialyl Lewis x (sLe^x) carbohydrates on PMNs completely prevented PMN transmigration (Fig. 6*C*, *D*), implying that additional molecules [*e.g.*, unknown glycoproteins on lipids (34)] may be involved in mediating PMN TEM.

DISCUSSION

Different families of adhesion molecules have been reported to participate in leukocyte–endothelium interactions, one of the key processes that occur during inflammation. P- and E-selectins are known to be involved in PMN capturing and rolling during this process. Using an *in vitro* PMN transmigration assay, we demonstrated the dynamic roles of E- and P-selectins in PMN transmigration. Four key points were highlighted by the results of this work: *1*) P- and E-selectins engage their common ligand PSGL-1 to activate β_2-integrins, thereby initiating PMN transmigration immediately after being plated on HUVECs (Figs. 3 and 4); *2*) E-selectin engages CD44 to activate β_2-integrins and influences PMN transmigration after 15 min of adding to the PMNs (Figs. 3 and 4), in which the binding affinities of P-selectin–PSGL-1, E-selectin–PSGL-1, and E-selectin–CD44 account for their differential contributions to PMN transmigration (Supplemental Figs. S3 and S4); *3*) all P- and E-selectin induced β_2-integrin activation is conducted through the Syk signaling pathway (Fig. 3*E*, *F*); and *4*) complicated complementary and competitive mechanisms are involved in the interactions between P-/E-selectins and their ligands to promote PMN transmigration (Fig. 5 and Supplemental Figs. S4 and S5). To our knowledge, these findings are novel in elucidating the dynamic PMN transmigration mediated by P-/E-selectins and β_2-integrins.

P- and E-selectins are expressed on activated endothelial cells (35). Previous studies have mainly focused on their roles in mediating leukocyte capturing and rolling. Our results indicate that P- and E-selectins can also engage CD44 or PSGL-1 to increase PMN transmigration by activating β_2-integrin (Fig. 3). Although PSGL-1 and CD44 are the major ligands for P- and E-selectin in mediating PMN transmigration, blocking CD44 alone (Fig. 5*A*, *B*) did not have a significant effect on the transmigration, but blocking PSGL-1 alone (Fig. 5*C*, *D*) significantly reduced the transmigration, especially before 15 min. These results suggest that E-/P-selectin and their ligands likely play complementary and competitive roles in promoting PMN transmigration, in that P-/E-selectin-PSGL-1 interaction plays a dominant role and E-selectin-CD44 has a complementary effect in this complicated competition for PMN transmigration on HUVECs. These findings are consistent with the previous observation that CD44 binds to E-selectin with a low affinity and that most molecules lack the proper glycosylation to bind to E-selectin (22).

Murine PMNs roll on E-selectin through their interactions with CD44, PSGL-1, ESL-1 (35) and an unknown *O*-glycosylated protein (22), but ESL-1 has not been detected on human PMNs and lymphocytes (1). The lectin domain of E-selectin binds to sLe^x [NeuAcα2-3Galβ1-4(Fucα1-3) GlcNAcβ1-R], a tetrasaccharide that caps the *N*-glycans on

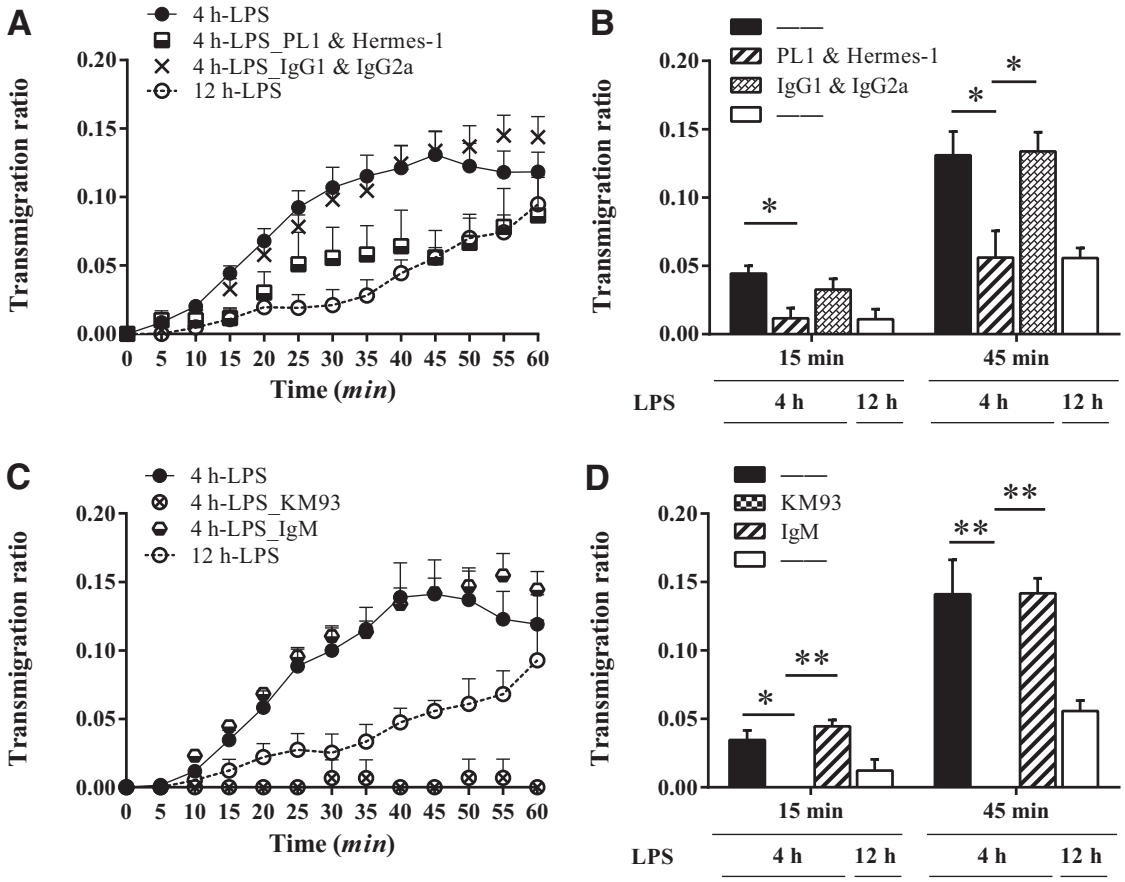

Figure 6. Complete inhibition of PMN transmigration *via* sLe^x blockage. *A*) Dynamic time course of transmigration ratio for PMNs incubated with the anti-PSGL-1 blocking mAb PL1 and the anti-CD44 mAb Hermes-1 on a 4-h LPS-treated HUVEC monolayer. Isotype-matched irrelevant mAbs (IgG1and IgG2a) were used as the control. Data were collected in 8–17 independent experiments. *C*) Dynamic time courses of transmigration ratio for PMNs incubated with the anti-sLe^x mAb KM93 on the 4-h LPS-treated HUVEC monolayer. An isotype-matched irrelevant mAb (IgM) was used as the control. Data were collected in 4–11 independent experiments. Data for 4- or 12-h LPS-treatment are also presented in *A* and *B* for comparison. *B*, *D*) Typical PMN transmigration ratio at $t = 15$ and 45 min from *A* and *C* were compared using 1-way ANOVA, followed by Tukey *post hoc* test. Data are means ± SE. $^*P < 0.05$; $^{**}P < 0.01$.

CD44 and the core 1-derived *O*-glycans on PSGL-1 and other unknown glycoproteins. P-selectin also interacts with PSGL-1 (9). P-selectin binds with a higher affinity to the N-terminal region of PSGL-1 through cooperative interactions with sulfated tyrosines and other amino acids and with an adjacent sLe^x-capped *O*-glycan. sLe^x can cap N- and *O*-glycans on many proteins and glycans on lipids and also serves as a selectin ligand on PMNs (1). In our study, blocking sLe^x on PMNs completely prevented PMN transmigration (Fig. 6*C*, *D*), whereas simultaneously blocking CD11a and CD11b did not (Fig. 3*A*, *B*). These results not only verify the contribution of selectins and their ligand in β_2-induced PMN transmigration but also indicate that there are many other molecules involved in PMN transmigration, but not through activating β_2-integrin.

LPS is known to increase endothelial cell permeability and to affect PMN TEM (27). In our study, HUVECs were exposed to LPS for 4 and 8 h to induce different selectin expression. We found that PMN transmigration was enhanced compared with the control in the absence of LPS stimuli (Fig. 1*B*, *C*). To interpret the results that increased E- and P-selectin expression is responsible for the increased PMN transmigration, we must rule out possible effects of LPS treatment on HUVEC permeability (Fig. 1*D*). In the 12-h LPS-treated HUVEC monolayer, significantly higher permeability was shown than in the 4-h LPS-treated cells, suggesting that increased PMN transmigration on 4-h LPS-treated HUVECs should not be attributed to LPS-induced permeability.

In our study, we used soluble isoforms of various adhesion molecules, termed sP-selectin and sCD44, to isolate the independent contributions of P-/E-selectin–PSGL-1 and E-selectin–CD44 binding to PMN transmigration on a 4-h LPS-treated HUVEC monolayer. This design is physiologically significant: soluble isoforms of these adhesion molecules are likely generated by enzymatic cleavage at a site close to the membrane insertion point after cytokine stimulation. The levels of these soluble molecules in plasma are often altered in inflammatory states, including atherosclerosis, diabetes, and many cardiovascular diseases (36), wherein PMN adhesion and transmigration are often abnormal. Previous work has shown that soluble molecules in plasma regulate PMN adhesion

and migration on HUVECs (37). Our *in vitro* study showed that sP-selectin and sCD44 may profoundly affect interactions between PMNs and the endothelium (Fig. 4*A–D*) and suggests that changes in the levels of these soluble isoforms in diseases may have a significant effect on microvascular injury through modulating PMN adhesion and transmigration. On the other hand, compared to the outcome of tests with blocking antibodies, using soluble isoforms to competitively bind selectin or its ligand may not induce any other physiologic abnormalities, as expected. The effects of blocking PSGL-1 by the addition of soluble P-selectin (Fig. 4*C*, *D*) and blocking *via* PL-1 (Fig. 5C, D) were comparable in the current study.

ICAM-1 is a key endothelial receptor that functions as a ligand for β_2-integrins on the surface of leukocytes, promoting leukocyte spreading and migration. However, ICAM-1 also functions in other ways in addition to being an adhesive ligand, because its engagement and clustering on leukocytes generate signals within endothelial cells that promote TEM (38). Indeed, increased downstream RhoA activity by ICAM-1 clustering is widely considered to contribute to leukocyte TEM by weakening junctions (39–41). However, ICAM-1 expression by 12-h LPS-treated HUVECs is >4-fold higher than that on 4-h LPS-treated HUVECs, suggesting that ICAM-1 alone is not sufficient to support transmigration because signaling by adhesion molecules such as P- and E-selectin are also necessarily required, whereas the current study focused primarily on the signaling downstream of P- and E-selectin engagement of PSGL-1 and CD44 to activate PMN β_2-integrin, understanding how P- and E-selectin function, in that signaling receptors to regulate endothelial cell cytoskeletal reorganization and to promote PMN transmigration will be critical in future investigations.

A body of evidence demonstrates that selectin–ligand interactions are strongly dependent on shear forces. For instance, selectin bonds exhibit both slip and catch bonding features (42) and undergo conformational changes that decrease their off-rate under low tensile forces (43). It is also noted that PMN crawling and transmigration present both passive and active patterns that are mainly mediated, respectively, by external forces of blood shear and by internal forces of cytoskeletal remodeling. To balance external forces, both selectins and their ligands also must be properly anchored to the cytoskeleton (29, 44, 45). In the absence of shear force, preanchored selectin bonds and β_2-integrin bonds undergo internal forces applied from actin polymerization-dependent extension and myosin II-mediated contraction. Thus, our primary goal was to isolate the active PMN transmigration dynamics under static condition from those coupled dynamics under shear flow. Internal forces applied by the cytoskeleton to selectin–ligand interactions also facilitate β_2-integrin activation through an inside–out signaling pathway (*e.g.*, the Syk pathway). For example, blocking mAbs directed against P- and E-selectin induce a rise in endothelial Ca^{2+} and the rearrangements of endothelial cytoskeleton without flow (11). Ligand-induced LFA-1 activation may take place more readily when LFA-1 is subjected to internal forces (46). Meanwhile, several processes of integrin-associated adhesion have been assessed in the absence of shear forces or have been involved in the late phases of PMN adhesion and spreading after initial bidirectional integrin activation (47). In the current study, we are focusing on elucidating dynamic contributions of P- and E-selectin-induced β_2-integrin activation under internal forces using a flow-free assay that enables us to refine the active regulation of β_2-integrin activation on PMN transmigration. Future works will be conducted to compare the active regulation with the coupling of active and passive manipulations under shear flow. FJ

ACKNOWLEDGMENTS

This work was supported by National Natural Science Foundation of China Grants 31230027, 91539119 and 31270994; National Key Basic Research Foundation of China Grant 2011CB710904; Strategic Priority Research Program Grant XDA01030102; and National High Technology Research and Development Program of China Grant 2011AA020109. The authors declare no conflicts of interest.

AUTHOR CONTRIBUTIONS

M. Long and Y. Zhang developed the concept, designed the tests, and wrote the paper; Y. Gong and Y. Zhang performed the experiments; S. Feng conduct numerical simulation, and Y. Zhang, Y. Gong., X. Liu, and S. Lü analyzed the data.

REFERENCES

1. Zarbock, A., Ley, K., McEver, R. P., and Hidalgo, A. (2011) Leukocyte ligands for endothelial selectins: specialized glycoconjugates that mediate rolling and signaling under flow. *Blood* **118**, 6743–6751
2. Yang, L., Froio, R. M., Sciuto, T. E., Dvorak, A. M., Alon, R., and Luscinskas, F. W. (2005) ICAM-1 regulates neutrophil adhesion and transcellular migration of TNF-alpha-activated vascular endothelium under flow. *Blood* **106**, 584–592
3. Lawson, C., and Wolf, S. (2009) ICAM-1 signaling in endothelial cells. *Pharmacol. Rep.* **61**, 22–32
4. Muller, W. A. (1995) The role of PECAM-1 (CD31) in leukocyte emigration: studies in vitro and in vivo. *J. Leukoc. Biol.* **57**, 523–528
5. O'Brien, C. D., Lim, P., Sun, J., and Albelda, S. M. (2003) PECAM-1-dependent neutrophil transmigration is independent of monolayer PECAM-1 signaling or localization. *Blood* **101**, 2816–2825
6. Feng, D., Nagy, J. A., Pyne, K., Dvorak, H. F., and Dvorak, A. M. (2004) Ultrastructural localization of platelet endothelial cell adhesion molecule (PECAM-1, CD31) in vascular endothelium. *J. Histochem. Cytochem.* **52**, 87–101
7. Lou, O., Alcaide, P., Luscinskas, F. W., and Muller, W. A. (2007) CD99 is a key mediator of the transendothelial migration of neutrophils. *J. Immunol.* **178**, 1136–1143
8. McEver, R. P. (2002) Selectins: lectins that initiate cell adhesion under flow. *Curr. Opin. Cell Biol.* **14**, 581–586
9. McEver, R. P. (1994) Selectins. *Curr. Opin. Immunol.* **6**, 75–84
10. Kelly, M., Hwang, J. M., and Kubes, P. (2007) Modulating leukocyte recruitment in inflammation. *J. Allergy Clin. Immunol.* **120**, 3–10
11. Lorenzon, P., Vecile, E., Nardon, E., Ferrero, E., Harlan, J. M., Tedesco, F., and Dobrina, A. (1998) Endothelial cell E- and P-selectin and vascular cell adhesion molecule-1 function as signaling receptors. *J. Cell Biol.* **142**, 1381–1391
12. Bevilacqua, M. P., Nelson, R. M., Mannori, G., and Cecconi, O. (1994) Endothelial-leukocyte adhesion molecules in human disease. *Annu. Rev. Med.* **45**, 361–378
13. Milstone, D. S., Fukumura, D., Padgett, R. C., O'Donnell, P. E., Davis, V. M., Benavidez, O. J., Monsky, W. L., Melder, R. J., Jain, R. K., and

Gimbrone, M. A., Jr. (1998) Mice lacking E-selectin show normal numbers of rolling leukocytes but reduced leukocyte stable arrest on cytokine-activated microvascular endothelium. *Microcirculation* **5**, 153–171
14. Yoshida, M., Westlin, W. F., Wang, N., Ingber, D. E., Rosenzweig, A., Resnick, N., and Gimbrone, M. A., Jr. (1996) Leukocyte adhesion to vascular endothelium induces E-selectin linkage to the actin cytoskeleton. *J. Cell Biol.* **133**, 445–455
15. Kaplanski, G., Farnarier, C., Benoliel, A. M., Foa, C., Kaplanski, S., and Bongrand, P. (1994) A novel role for E- and P-selectins: shape control of endothelial cell monolayers. *J. Cell Sci.* **107**, 2449–2457
16. Hynes, R. O. (2002) Integrins: bidirectional, allosteric signaling machines. *Cell* **110**, 673–687
17. Li, N., Mao, D., Lü, S., Tong, C., Zhang, Y., and Long, M. (2013) Distinct binding affinities of Mac-1 and LFA-1 in neutrophil activation. *J. Immunol.* **190**, 4371–4381
18. Shimaoka, M., Xiao, T., Liu, J. H., Yang, Y., Dong, Y., Jun, C. D., McCormack, A., Zhang, R., Joachimiak, A., Takagi, J., Wang, J. H., and Springer, T. A. (2003) Structures of the alpha L I domain and its complex with ICAM-1 reveal a shape-shifting pathway for integrin regulation. *Cell* **112**, 99–111
19. Mao, D., Lü, S., Li, N., Zhang, Y., and Long, M. (2011) Conformational stability analyses of alpha subunit I domain of LFA-1 and Mac-1. *PLoS One* **6**, e24188
20. Zarbock, A., Kempf, T., Wollert, K. C., and Vestweber, D. (2012) Leukocyte integrin activation and deactivation: novel mechanisms of balancing inflammation. *J. Mol. Med.* **90**, 353–359
21. Yago, T., Shao, B., Miner, J. J., Yao, L., Klopocki, A. G., Maeda, K., Coggeshall, K. M., and McEver, R. P. (2010) E-selectin engages PSGL-1 and CD44 through a common signaling pathway to induce integrin alphaLbeta2-mediated slow leukocyte rolling. *Blood* **116**, 485–494
22. Yago, T., Fu, J., McDaniel, J. M., Miner, J. J., McEver, R. P., and Xia, L. (2010) Core 1-derived O-glycans are essential E-selectin ligands on neutrophils. *Proc. Natl. Acad. Sci. USA* **107**, 9204–9209
23. Wang, H. B., Wang, J. T., Zhang, L., Geng, Z. H., Xu, W. L., Xu, T., Huo, Y., Zhu, X., Plow, E. F., Chen, M., and Geng, J. G. (2007) P-selectin primes leukocyte integrin activation during inflammation. *Nat. Immunol.* **8**, 882–892
24. Simon, S. I., Burns, A. R., Taylor, A. D., Gopalan, P. K., Lynam, E. B., Sklar, L. A., and Smith, C. W. (1995) L-selectin (CD62L) cross-linking signals neutrophil adhesive functions via the Mac-1 (CD11b/CD18) beta 2-integrin. *J. Immunol.* **155**, 1502–1514
25. Chatterjee, A., Gogolak, P., Blottière, H. M., and Rajnavölgyi, É. (2015) The impact of ATRA on shaping human myeloid cell responses to epithelial cell-derived stimuli and on T-lymphocyte polarization. *Mediators Inflamm.* **2015**, 579830
26. Eutamene, H., Theodorou, V., Schmidlin, F., Tondereau, V., Garcia-Villar, R., Salvador-Cartier, C., Chovet, M., Bertrand, C., and Bueno, L. (2005) LPS-induced lung inflammation is linked to increased epithelial permeability: role of MLCK. *Eur. Respir. J.* **25**, 789–796
27. Williams, M., Blocksom, J. M., Kerkar, S., Steffes, C. P., Tyburski, J. G., Carlin, A. M., and Wilson, R. F. (2003) LPS increases permeability of rat lung microvascular endothelial cell-pericyte cocultures (abstract). *Crit. Care Med.* **31**, A45
28. Ma, Y. Q., Plow, E. F., and Geng, J. G. (2004) P-selectin binding to P-selectin glycoprotein ligand-1 induces an intermediate state of alphaMbeta2 activation and acts cooperatively with extracellular stimuli to support maximal adhesion of human neutrophils. *Blood* **104**, 2549–2556
29. Miner, J. J., Xia, L., Yago, T., Kappelmayer, J., Liu, Z., Klopocki, A. G., Shao, B., McDaniel, J. M., Setiadi, H., Schmidtke, D. W., and McEver, R. P. (2008) Separable requirements for cytoplasmic domain of PSGL-1 in leukocyte rolling and signaling under flow. *Blood* **112**, 2035–2045
30. Zarbock, A., Abram, C. L., Hundt, M., Altman, A., Lowell, C. A., and Ley, K. (2008) PSGL-1 engagement by E-selectin signals through Src kinase Fgr and ITAM adapters DAP12 and FcR gamma to induce slow leukocyte rolling. *J. Exp. Med.* **205**, 2339–2347
31. Norman, K. E., Moore, K. L., McEver, R. P., and Ley, K. (1995) Leukocyte rolling in vivo is mediated by P-selectin glycoprotein ligand-1. *Blood* **86**, 4417–4421
32. Katayama, Y., Hidalgo, A., Chang, J., Peired, A., and Frenette, P. S. (2005) CD44 is a physiological E-selectin ligand on neutrophils. *J. Exp. Med.* **201**, 1183–1189
33. Nácher, M., Blázquez, A. B., Shao, B., Matesanz, A., Prophete, C., Berin, M. C., Frenette, P. S., and Hidalgo, A. (2011) Physiological contribution of CD44 as a ligand for E-selectin during inflammatory T-cell recruitment. *Am. J. Pathol.* **178**, 2437–2446
34. Laszik, Z., Jansen, P. J., Cummings, R. D., Tedder, T. F., McEver, R. P., and Moore, K. L. (1996) P-selectin glycoprotein ligand-1 is broadly expressed in cells of myeloid, lymphoid, and dendritic lineage and in some nonhematopoietic cells. *Blood* **88**, 3010–3021
35. McEver, R. P., and Zhu, C. (2010) Rolling cell adhesion. *Annu. Rev. Cell Dev. Biol.* **26**, 363–396
36. Roldán, V., Marín, F., Lip, G. Y., and Blann, A. D. (2003) Soluble E-selectin in cardiovascular disease and its risk factors: a review of the literature. *Thromb. Haemost.* **90**, 1007–1020
37. Ohno, N., Ichikawa, H., Coe, L., Kvietys, P. R., Granger, D. N., and Alexander, J. S. (1997) Soluble selectins and ICAM-1 modulate neutrophil-endothelial adhesion and diapedesis in vitro. *Inflammation* **21**, 313–324
38. Allingham, M. J., van Buul, J. D., and Burridge, K. (2007) ICAM-1-mediated, Src- and Pyk2-dependent vascular endothelial cadherin tyrosine phosphorylation is required for leukocyte transendothelial migration. *J. Immunol.* **179**, 4053–4064
39. Sans, E., Delachanal, E., and Duperray, A. (2001) Analysis of the roles of ICAM-1 in neutrophil transmigration using a reconstituted mammalian cell expression model: implication of ICAM-1 cytoplasmic domain and Rho-dependent signaling pathway. *J. Immunol.* **166**, 544–551
40. Wittchen, E. S. (2009) Endothelial signaling in paracellular and transcellular leukocyte transmigration. *Front. Biosci. (Landmark Ed.)* **14**, 2522–2545
41. Adamson, P., Etienne, S., Couraud, P. O., Calder, V., and Greenwood, J. (1999) Lymphocyte migration through brain endothelial cell monolayers involves signaling through endothelial ICAM-1 via a rho-dependent pathway. *J. Immunol.* **162**, 2964–2973
42. Marshall, B. T., Long, M., Piper, J. W., Yago, T., McEver, R. P., and Zhu, C. (2003) Direct observation of catch bonds involving cell-adhesion molecules. *Nature* **423**, 190–193
43. Zhu, C., Lou, J., and McEver, R. P. (2005) Catch bonds: physical models, structural bases, biological function and rheological relevance. *Biorheology* **42**, 443–462
44. Alon, R., and Dustin, M. L. (2007) Force as a facilitator of integrin conformational changes during leukocyte arrest on blood vessels and antigen-presenting cells. *Immunity* **26**, 17–27
45. Cairo, C. W., Mirchev, R., and Golan, D. E. (2006) Cytoskeletal regulation couples LFA-1 conformational changes to receptor lateral mobility and clustering. *Immunity* **25**, 297–308
46. Varma, R., Campi, G., Yokosuka, T., Saito, T., and Dustin, M. L. (2006) T cell receptor-proximal signals are sustained in peripheral microclusters and terminated in the central supramolecular activation cluster. *Immunity* **25**, 117–127
47. Alon, R., Grabovsky, V., and Feigelson, S. (2003) Chemokine induction of integrin adhesiveness on rolling and arrested leukocytes local signaling events or global stepwise activation? *Microcirculation* **10**, 297–311

Received for publication March 20, 2016.
Accepted for publication September 22, 2016.

Dynamic contributions of P- and E-selectins to β_2-integrin induced neutrophil transmigration

Yixin Gong, Yan Zhang, Shiliang Feng, et al.

FASEB J published online October 6, 2016
Access the most recent version at doi:10.1096/fj.201600398RRR

SUPPLEMENTAL MATERIALS

Table of contents

MODEL FORMULATION

The model is developed from literatures (1, 2). The two-dimensional cell (PMN) cytoskeleton is discreted by *N* nodes upon Delaunay triangulation (**Fig. S3*B***). Each edge that connects neighboring nodes *i* and *j* consists of an elastic Hooke spring. A sliding friction element accounting for viscous dissipation effect associated with cytoskeleton-fluid friction. Initially, each node is equally assigned with PSGL-1, CD44, and β_2-integrin (activated or inactivated). P-selectin, E-selectin, and ICMA-1 are uniformly distributed on endothelial cell with well defined stiffness, E_s (**Supplemental Table S1**). The model is divided into two modules, named as cell mechanics and integrin dynamic activation, respectively.

Cell Mechanics

There are three types of forces acting on each node *i*, substrate frictional drag force ($\overrightarrow{F_i^{\text{drag}}}$), passive elastic force ($\overrightarrow{F_i^{\text{int}}}$), and active force ($\overrightarrow{F_i^{\text{act}}}$), to expound cell's movement:

$$\overrightarrow{F_i^{\text{drag}}} + \overrightarrow{F_i^{\text{int}}} = \overrightarrow{F_i^{\text{act}}}. \tag{S1}$$

$\overrightarrow{F_i^{\text{drag}}}$ is composed of two parts:

$$\overrightarrow{F_i^{\text{drag}}} = \eta \frac{\partial \overrightarrow{u_i}}{\partial t} + \sum_{g=1}^{4} \sum_{q=1}^{N_{i,g}^{\text{b}}} \overrightarrow{r_{q,g}^{i}} K_{\text{tot}} \tag{S2}$$

Here, η is the drag coefficient, $\overrightarrow{u_i}$ is the displacement vector, and the second term on the right denotes the resistance force arisen from the stretch of receptor-ligand bonds （*i.e.*, P-sel-PSGL-1, E-sel-PSGL-1, E-sel-CD44, and β_2-integrin-ICAM-1. $\overrightarrow{r_{q,g}^{i}}$ is the displacement vector of each bond *q* of the *g-th* interacting pair (*g* = 1, 2, 3, 4), and $N_{i,g}^{\text{b}}$ is the total number of bonds. K_{tot} represents the effective spring constant and is calculated by $1/K_{\text{tot}} = 1/K_{\text{s}} + 1/K_{\text{c}}$, where K_{s} and K_{c} are spring constants of endothelial cells (acting as substrate) and force-bearing intracellular structures (*i.e.*, selectin-ligand bonds and β_2-integrin-ligand bonds), respectively.

$\overrightarrow{F_i^{\text{int}}}$ in Eq. S1 represents the sum of elastic stress at node *i* with *j* = 1, 2, 3…G_i neighboring nodes, can be written as:

$$\overrightarrow{F_i^{\text{int}}} = \sum_{j=1}^{G_i} (E_{ij}\varepsilon_{ij}) r_{ij}, \tag{S3}$$

where r_{ij} is the unit vector parallel to the connecting edge, and ε_{ij} is the linear deformation of the spring between neighboring nodes *i* and *j*, E_{ij} is the element elastic modules, which can be estimated from the typical elastic modules of cell cytoskeleton (E_0), and G_i is the number of elements through the *i-th* node.

$\overrightarrow{F_i^{\text{act}}}$ terms the active forces, which mainly refers to F-actin polymerization force that is transduced to endothelial cells *via* engaged β_2-integrins bonds (g = 4). The magnitude dependence of $\overrightarrow{F_i^{\text{act}}}$ on PMN-endothelial cell adhesion strength is described by the following Langmuir–Hill equation:

$$\overrightarrow{F_i^{\text{act}}} = \frac{F_{\text{M}}}{N_{\text{front}}}\left(\frac{(N_{i,4}^{\text{b}})^2}{(N_{\text{opt}})^2+(N_{i,4}^{\text{b}})^2}\right)\hat{l}_{ic}, \tag{S4}$$

where F_{M} is the maximum active force generated by a single PMN, N_{front} is the number of nodes at the frontal region. N_{opt} is the typical number of engaged β_2-integrin-ICAM-1 bonds. $\hat{l}_i$ is the unit vector parallel to the line connecting cell center to the *i-th* frontal node.

Integrin dynamic activation

In our model, activated β_2-integrin-ICAM-1 interactions mediate cell adhesion and movement. Dynamic activation of β_2-integrin is controlled by the interactions of E- and P-selectins with their ligands (*e.g.*, E-sel-PSGL-1, P-sel-PSGL-1, and E-sel-CD44) in a force-dependent manner. Bond formation is described by a stochastic process due to respective receptor-ligand binding kinetics (**Supplemental Table S1**). A general one-step multivalent reversible reaction can be written as:

$$\nu^{\text{r}} m_{\text{r}} + \nu^{\text{l}} m_{\text{l}} \underset{k_{\text{off}}}{\overset{k_{\text{on}}}{\rightleftharpoons}} \nu^{\text{b}} m_{\text{b}}, \tag{S5}$$

Where m_{r} (P-selectin, E-selectin, and β_2-integrin), m_{l} (PSGL-1, CD44, and ICAM-1), and m_{b} (P-sel-PSGL-1, E-sel-PSGL-1, E-sel-CD44, and β_2-integrin-ICAM-1) denote receptor, ligand, and receptor-ligand bonds, respectively. ν^{r}, ν^{l}, and ν^{b} denote the corresponding stoichiometric coefficients (ν^{r} = ν^{l} = ν^{b} = 1 in the current work). k_{off} is the off-rate and is updated after each simulation time interval (Δt) according to the Bell model (3). k_{on} is the on-rate.

We define a threshold force beyond which β_2-integrins are activated. For each node, the variation in the number of activated β_2-integrin (δA_i) in each time interval is calculated as:

$$\delta A_i = S_i - \gamma A_i \Delta t, \tag{S6}$$

Where γ is the self-inactivation rate of β_2-integrin. S_i is the source term defined as:

$$S_i = \begin{cases} S_0 \Delta t + \kappa N_T^i \delta\rho & \text{if } f_q^i \geq F_r \text{ and } \sum_T^{T+n} N_T^i \leq N_{max} \\ S_0 \Delta t & \text{if } f_q^i < F_r \end{cases}, \tag{S7}$$

where S_0 is the basal rate of β_2-integrin activation, $\delta\rho$ is the rate of P- or E-selectin mediated β_2-integrin activation, F_r is the threshold force, f_q^i is the force on ligand-engaged bond, N_T is the number of binding events at current time step that may induce β_2-integrin activation, N_{max} is the maximum number of β_2-integrin activation events during *n* steps, and κ is a limiting factor due to the pool of inactivated β_2-integrins, and is given by,

$$\kappa = \frac{N_{tot} - N_{act}(t)}{N_{tot} - N_{ini}}, \tag{S8}$$

Where N_{tot} is the total number of β_2-integrin (activated plus inactivated), N_{ini} is the initial number of activated β_2-integrin, and $N_{act}(t)$ is the total number of activated β_2-integrin at present.

NUMERICAL IMPLEMENTATION

The master equations (Eqs. S1 and S5) were numerically solved with respective finite element method (FEM) and Monte-Carlo simulation (MCS) with a time step (Δt) of 0.02 s. As many signaling components may be involved in E- and P-selectin mediated β_2-integrin activation, the real situation is much complex than the above theoretical description. We take the following criteria to run our model: if the input force is at appropriate intensity, the activation rate of β_2-integrins is positively correlated with force strength; however, if the input signal becomes too intense, the concentration of intermediate signaling components, *i.e.*, Syk, reach saturation to prevent infinite β_2-integrin activation.

SUPPLEMENTAL FIGURES

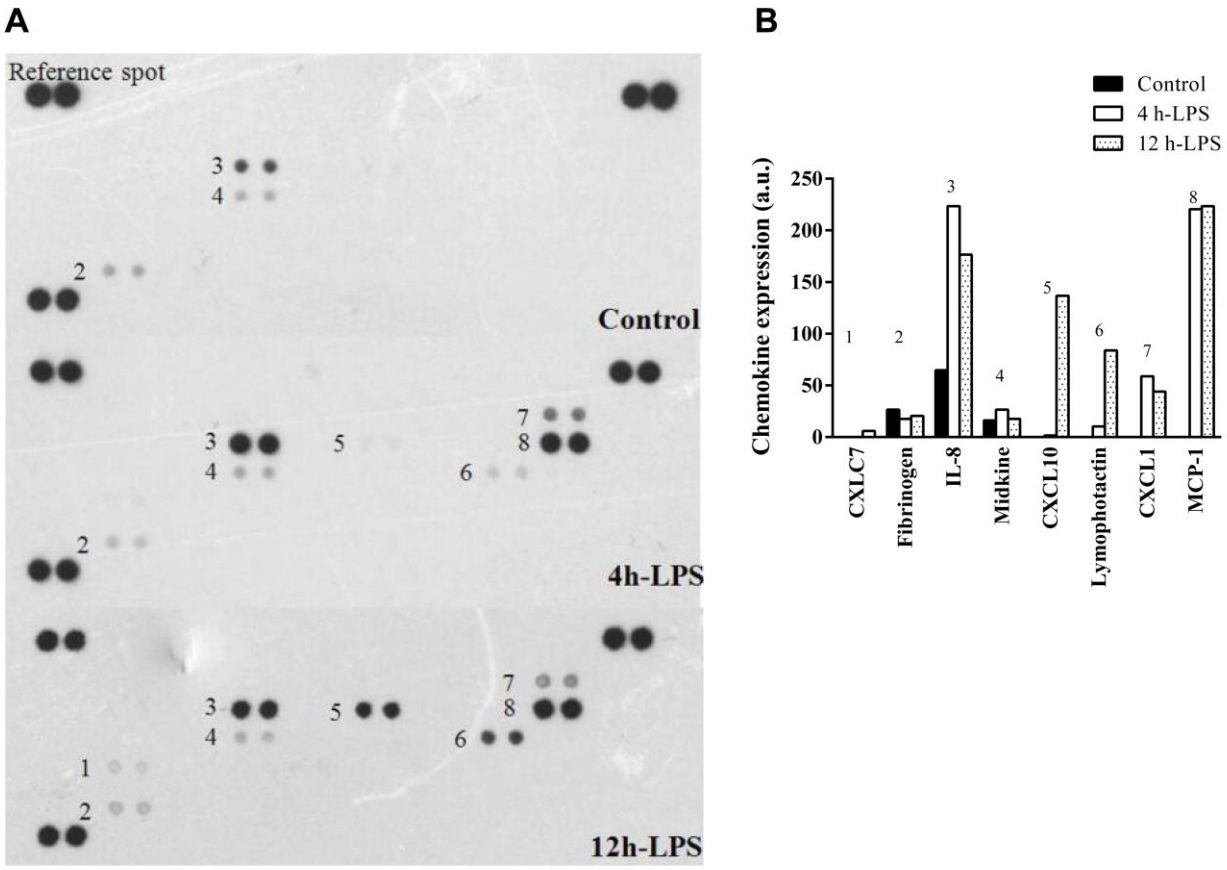

Figure S1. Chemokine microarray for culture supernates from untreated or LPS-treated HUVECs. *A*) Localization of chemokine probes in the membranes related to positive controls and reference spots. *B*) Relative expression levels of chemokines measured by densitometry.

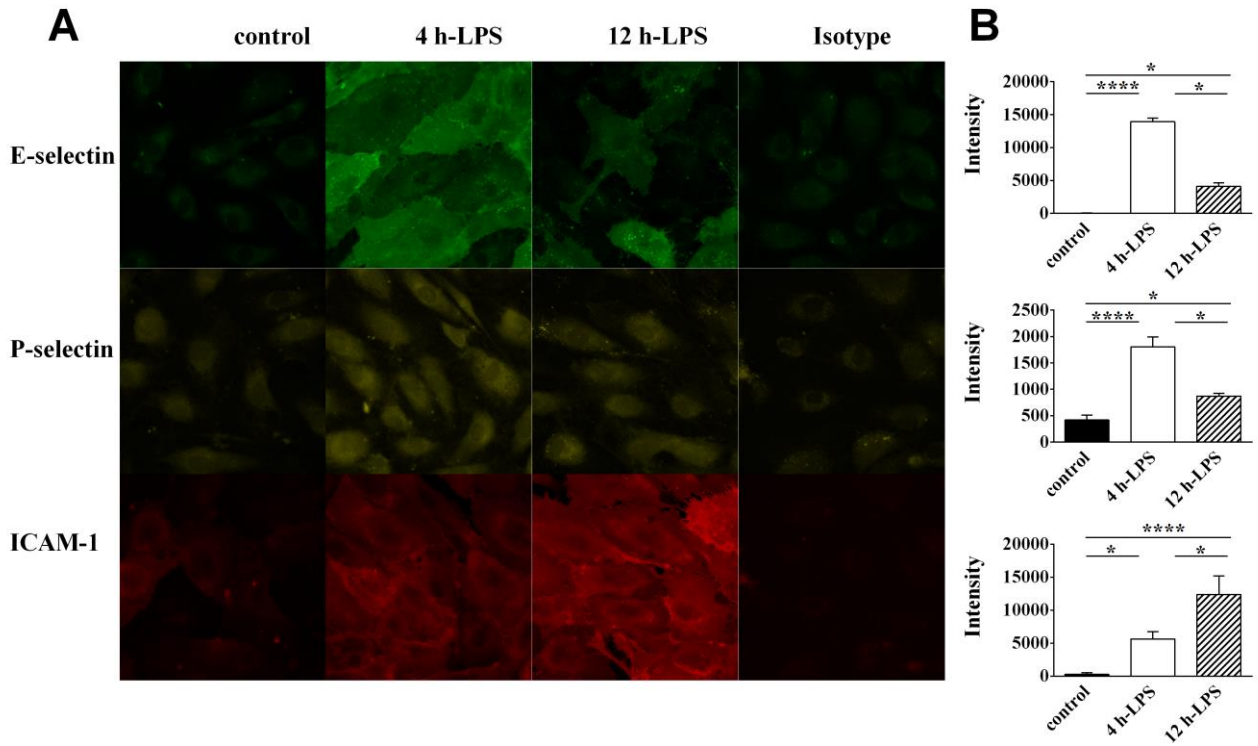

Figure S2. Selectin expression is increased on 4 h LPS-treated HUVEC monolayer. Fluorescent images of HUVEC monolayer treated with culture media containing 1 μg/ml LPS for 4 or 12 h or culture media alone (control) and then stained with respective mAbs or corresponding isotype-matched irrelevant mAbs. Compared to intact cells (no LPS treatment), E-selectin expression peaked at 4 h LPS-treated HUVECs, increasing 2.37-fold (fluorescence intensity (FI) increased from 4835 to 11478) and returning to baseline (FI = 5610) within 12 h. P-selectin expression on 4 h LPS-treated HUVECs increased by approximately 30% (*i.e.*, FI increased from 2025 to 2635) and returned to baseline (FI = 2154) within 12 h. However, ICAM-1 expression increased with increasing LPS treatment duration; FI increased from 269 (0 h) to 6009 (4 h) and peaked at 12 h with FI = 25251. Data were collected from 9-10 independent experiments. All data were compared using one-way ANOVA followed by Tukey post-hoc test and presented as the mean ± SE. $^{*}P<0.05$; $^{****}P<0.0001$.

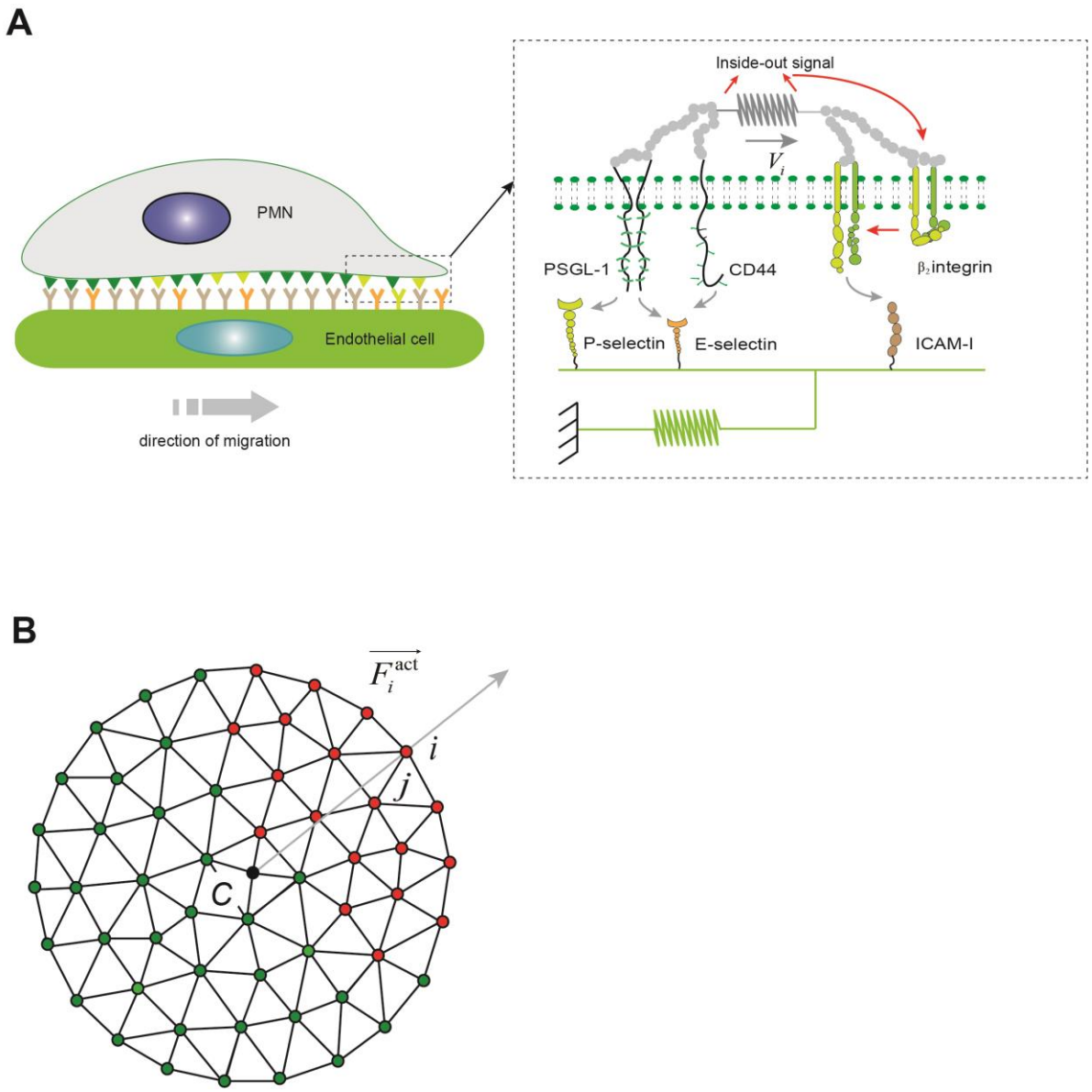

Figure S3. Illustration of a two-dimensional theoretical model. *A*) Side-view schematic of PMN-endothelial cell system. The rectangular region of the lamellipodia is magnified to display specific molecular interactions involved in current study. Activation of β_2-integrins is induced by ligand-engaged selectin bonds in a force dependent manner, where PSGL-1 and CD44 on PMN competitively bind with E-selectin while PSGL-1 may also bind with P-selectin on endothelial cell. *B*) Top-view of finite element model of the lamellipod. The lamellipodia is triangulated, such that each node represents a mass of cytoskeleton contained in the surrounding Voronoi polygon. Active force, mainly referring to F-actin polymerization force, is applied only at nodes marked by red dots.

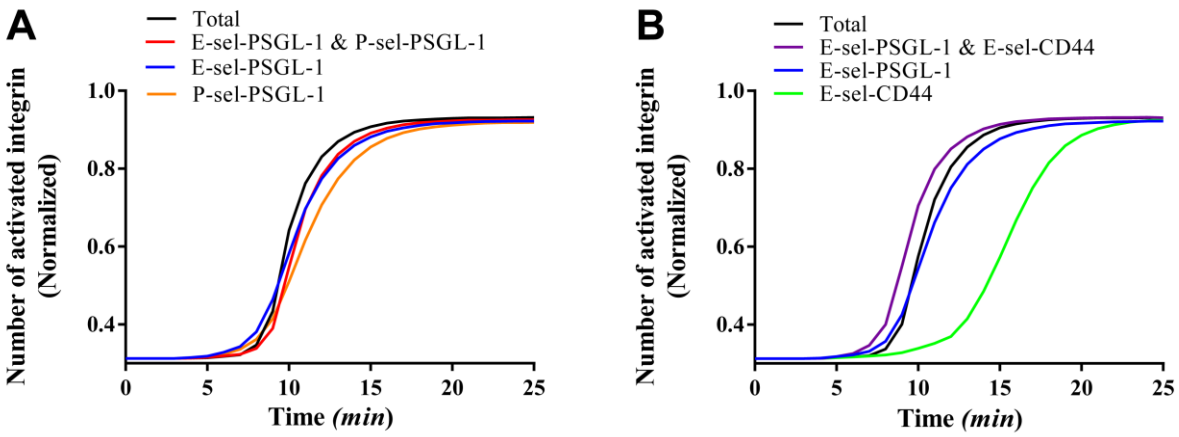

Figure S4. Complementary and competitive roles of ligand-engaged selectin bonds induced β_2-integrin activation. Numerical simulations of time-dependent evolution of β_2-integrin activation are shown in the two cases of *A*) E- and P-selectin respectively or competitively binding to PSLG-1 and *B*) PSGL-1 and CD44 respectively or competitively binding to E-selectin. All data were collected from 30 independent simulations.

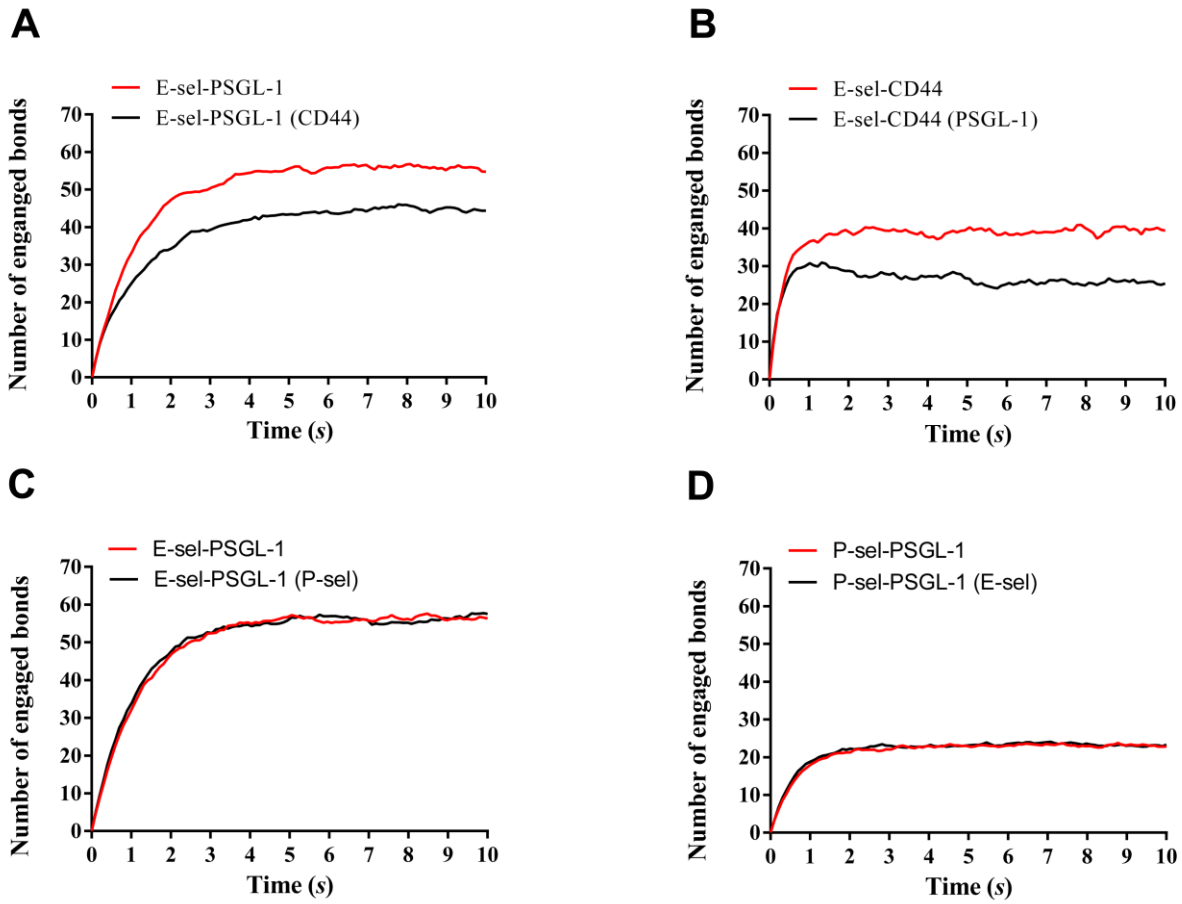

Figure S5. Time-dependent evolution of the number of engaged E/P-selectin -PSGL-1 and E-selectin-CD44 bonds. *A*) Number of engaged E-selectin-PSGL-1 bonds upon PSGL-1 sole-expression (red line) and PSGL-1/CD44 (black line) co-engaged conditions. *B*) Number of engaged E-selectin-CD44 bonds under CD44 sole-engaged (red line) and PSGL-1/CD44 co-engaged (black line) conditions. Due to the limitation of E-selectin, the number of engaged E-selectin-PSGL-1 bond has been significantly decreased in PSGL-1/CD44 co-expression condition, and so is the number of engaged E-selectin-CD44 bonds, suggesting that CD44 may compete with PSGL-1 for E-selectin. *C*) Number of engaged E-selectin-PSGL-1 bonds upon E-selectin sole-expression (red line) and E/P-selectin co-engaged conditions (black line). *D*) Corresponding P-selectin-PSGL-1 bond number. All data were collected from 30 independent simulations.There is no significant difference in sole- or co-engaged conditions due to adequate expression of PSGL-1. All simulations were conducted at A_c = 1 μm and zero force (***cf.* Supplemental Table S1**).

SUPPLEMENTAL TABLE

Supplemental Table S1. Kinetic parameters used for calculations

Parameter description	Symbol	Value	Sources
Young's modulus of endothelial cell	E_s	5 kPa	(4, 5)
Young's modulus of PMN	E_0	5 kPa	(4, 5)
Clutch spring constant	K_C	1 nN·nm^{-1}	(3, 6)
Viscosity constant	η	30 pN min ·μm^{-3}	(5, 7)
Total amount of activate force	F_M	20 nN	(1)
Threshold force	F_r	10 pN	Assumed upon (3)
Cell radius	r_m	5 μm	This work
Compliance length	λ	0.1 nm	(8)
Mechanical feedback strength	δρ	0.5	Assumed upon (3)
Total integrin number	N_{tot}	8000	This work
Densities of PSGL-1 and CD44	ρ_p, ρ_c	388, 1788 molecules/μm^2	This work
Densities of E-selectin, P-selectin, and ICMA-1	ρ_{ES}, ρ_{pS}, ρ_1	129, 33, 200 molecules/μm^2	This work
Kinetic parameters of E-selectin-PSGL-1 binding	$A_c k_f^0$, k_r^0	10^{-3}μm^4/s 0.5 s^{-1}	(9)
Kinetic parameters of E-selectin-CD44 binding	$A_c k_f^0$, k_r^0	5×10^{-4}μm^4/s 2.0 s^{-1}	Assumed upon (10)
β_2-integrin / ICAM-1 kinetics	$A_c k_f^0$, k_r^0	10^{-5}μm^4/s 1.0 s^{-1}	(11)
P-selectin/PSGL-1 kinetics	$A_c k_f^0$, k_r^0	3×10^{-3}μm^4/s	(9)

		1.0 s^{-1}	

REFERENCES:

1. Dokukina, I. V., and Gracheva, M. E. (2010) A Model of Fibroblast Motility on Substrates with Different Rigidities. *Biophys. J.* **98**, 2794-2803
2. Elosegui-Artola, A., Bazellieres, E., Allen, M. D., Andreu, I., Oria, R., Sunyer, R., Gomm, J. J., Marshall, J. F., Jones, J. L., Trepat, X., and Roca-Cusachs, P. (2014) Rigidity sensing and adaptation through regulation of integrin types. *Nat. Mater.* **13**, 631-637
3. Kong, D., Ji, B. H., and Dai, L. H. (2010) Stabilizing to disruptive transition of focal adhesion response to mechanical forces. *J. Biomech.* **43**, 2524-2529
4. Schwarz, U. S., Erdmann, T., and Bischofs, I. B. (2006) Focal adhesions as mechanosensors: The two-spring model. *Biosystems* **83**, 225-232
5. Ghibaudo, M., Saez, A., Trichet, L., Xayaphoummine, A., Browaeys, J., Silberzan, P., Buguin, A., and Ladoux, B. (2008) Traction forces and rigidity sensing regulate cell functions. *Soft. Matter.* **4**, 1836-1843
6. Roca-Cusachs, P., Iskratsch, T., and Sheetz, M. P. (2012) Finding the weakest link-exploring integrin-mediated mechanical molecular pathways. *J. Cell Sci.* **125**, 3025-3038
7. Borau, C., Kamm, R. D., and Garcia-Aznar, J. M. (2011) Mechano-sensing and cell migration: a 3D model approach. *Phys. Biol.* **8**, 1347-1371
8. Zhong, Y., and Ji, B. (2014) How do cells produce and regulate the driving force in the process of migration? *Eur. Phys. J-Spec. Top.* **223**, 1373-1390
9. Wu, L., Xiao, B. T., Jia, X. L., Zhang, Y., Lu, S. Q., Chen, J., and Long, M. (2007) Impact of carrier stiffness and microtopology on two-dimensional kinetics of P-selectin and P-selectin glycoprotein ligand-1 (PSGL-1) interactions. *J. Biol. Chem.* **282**, 9846-9854
10. Wang, Y., Yago, T., Zhang, N., Abdisalaam, S., Alexandrakis, G., Rodgers, W., and McEver, R. P. (2014) Cytoskeletal Regulation of CD44 Membrane Organization and Interactions with E-selectin. *J Biol Chem* **289**, 35159-35171
11. Zhang, F., Marcus, W. D., Goyal, N. H., Selvaraj, P., Springer, T. A., and Zhu, C. (2005) Two-dimensional kinetics regulation of alpha(L)beta(2)-ICAM-1 interaction by conformational changes of the alpha(L)-inserted domain. *J. Biol. Chem.* **280**, 42207-42218